An Enantioselective Synthetic Route toward Second-Generation Light-Driven Rotary Molecular Motors

ARTICLE *in* THE JOURNAL OF ORGANIC CHEMISTRY · FEBRUARY 2010

Impact Factor: 4.72 · DOI: 10.1021/jo902348u · Source: PubMed

7 AUTHORS, INCLUDING:

Frédéric Dumur
Aix-Marseille Université
158 PUBLICATIONS **1,879** CITATIONS
SEE PROFILE

Auke Meetsma
University of Groningen
527 PUBLICATIONS **15,631** CITATIONS
SEE PROFILE

JOC Article
pubs.acs.org/joc

An Enantioselective Synthetic Route toward Second-Generation Light-Driven Rotary Molecular Motors

Thomas C. Pijper, Dirk Pijper, Michael M. Pollard, Frédéric Dumur, Stephen G. Davey, Auke Meetsma, and Ben L. Feringa*

Stratingh Institute for Chemistry, Zernike Institute for Advanced Materials, and Center for Systems Chemistry, University of Groningen, Nijenborgh 4, 9747 AG, Groningen, The Netherlands

b.l.feringa@rug.nl

Received November 6, 2009

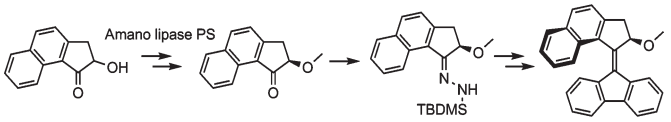

Controlling the unidirectional rotary process of second-generation molecular motors demands access to these motors in their enantiomerically pure form. In this paper, we describe an enantioselective route to three new second-generation light-driven molecular motors. Their synthesis starts with the preparation of an optically active α-methoxy-substituted upper-half ketone involving an enzymatic resolution. The subsequent conversion of this ketone to the corresponding hydrazone by treatment with hydrazine led to full racemization. However, conversion to a TBDMS-protected hydrazone by treatment with bis-TBDMS hydrazine, prepared according to a new procedure, proceeds with nearly full retention of the stereochemical integrity. Oxidation of the TBDMS-protected hydrazone and subsequent coupling to a lower-half thioketone followed by recrystallization provided the molecular motors with >99% ee. As these are the first molecular motors that have a methoxy substituent at the stereogenic center, the photochemical and thermal isomerization steps involved in the rotary cycle of one of these new molecules were studied in detail with various spectroscopic techniques.

Introduction

The bottom-up construction of nanoscale devices in which motion can be induced and/or controlled at the molecular level is a topic of great contemporary interest.[1] Inspired by the highly sophisticated and effective molecular devices that are present in nature, such as the bacterial flagellum and the ATP synthase rotary motors,[2] a wide array of such devices has been designed and studied in recent years.[3] Among these are various types of rotary molecular motors, which are capable of converting energy into rotary motion and which have a preference for a unique sense of rotation.[3] Our group has reported a series of rotary molecular motors that perform unidirectional rotation around an olefin axis upon irradiation with light.[4] Rotary molecular motors that are fueled by chemical energy are also known: Kelly and co-workers[5] and Branchaud and co-workers[6] have presented rotors which are capable of unidirectional 120 and 180° rotation, respectively, whereas we have reported a rotary motor which is capable of continuous, unidirectional 360° rotation.[7] In addition, two catenane systems which are able to undergo unidirectional rotation have been described by Leigh and co-workers.[8]

Two types of light-driven rotary molecular motors that are derived from overcrowded alkenes have been designed: the

(1) (a) *Molecular Devices and Machines: Concepts and Perspectives for the Nanoworld*; Balzani, V., Credi, A., Venturi, M., Eds.; Wiley-VCH: Weinheim, Germany, 2008. (b) van den Heuvel, M. G. L.; Dekker, C. *Science* **2007**, *317*, 333–336. (c) Whitesides, G. M. *Sci. Am.* **2001**, *285*, 78–83.

(2) *Molecular Motors* Schliwa, M., Ed.; Wiley-VCH: Weinheim, Germany, 2003.

(3) For reviews, see: (a) Kay, E. R.; Leigh, D. A.; Zerbetto, F. *Angew. Chem., Int. Ed.* **2007**, *46*, 72–191. (b) Browne, W. R.; Feringa, B. L. *Nat. Nanotechnol.* **2006**, *1*, 25–35. (c) Kottas, G. S.; Clarke, L. I.; Horinek, D.; Michl, J. *Chem. Rev.* **2005**, *105*, 1281–1376.

(4) For a comprehensive review, see: Feringa, B. L. *J. Org. Chem.* **2007**, *72*, 6635–6652.

(5) (a) Kelly, T. R.; De Silva, H.; Silva, R. A. *Nature* **1999**, *401*, 150–152. (b) Kelly, T. R.; Silva, R. A.; De Silva, H.; Jasmin, S.; Zhao, Y. *J. Am. Chem. Soc.* **2000**, *122*, 6935–6949. (c) Kelly, T. R.; Cavero, M. *Org. Lett.* **2002**, *4*, 2653–2656. (d) Kelly, T. R.; Cai, X.; Damkaci, F.; Panicker, S. B.; Tu, B.; Bushell, S. M.; Cornella, I.; Piggott, M. J.; Salives, R.; Cavero, M.; Zhao, Y.; Jasmin, S. *J. Am. Chem. Soc.* **2007**, *129*, 376–386.

(6) Lin, Y.; Dahl, B. J.; Branchaud, B. P. *Tetrahedron Lett.* **2005**, *46*, 8359–8362.

(7) Fletcher, S. P.; Dumur, F.; Pollard, M. M.; Feringa, B. L. *Science* **2005**, *310*, 80–82.

(8) (a) Leigh, D. A.; Wong, J. K. Y.; Dehez, F.; Zerbetto, F. *Nature* **2003**, *424*, 174–179. (b) Hernández, J. V.; Kay, E. R.; Leigh, D. A. *Science* **2004**, *306*, 1532–1537.

DOI: 10.1021/jo902348u Published on Web 01/07/2010

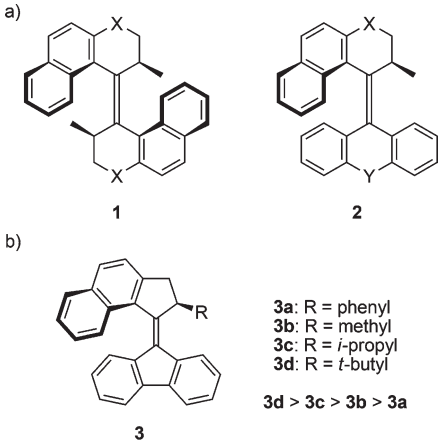

FIGURE 1. (a) First-generation molecular motor **1** and second-generation molecular motor **2**. (b) Molecular motor **3** with various substituents, in order of the enhanced rate of the thermal isomerization step.

first-generation type **1**,[9] which has an identical upper and lower half, and the second-generation type **2**,[10] which has a dissimilar upper and lower half (Figure 1a). Key features of these motors are the helical shape, the central olefin which is prone to stilbene-type photoisomerization and which serves as the axis of rotation, and the presence of a stereogenic center (two stereogenic centers in the case of the first-generation system) next to the central olefin. Rotation in these systems takes place through two photochemically driven, reversible *cis*−*trans* isomerizations of the central olefin, which are each followed by a thermally driven, irreversible helix inversion. The direction of this rotation is dictated by the absolute configuration of the stereogenic center(s). The rotational speed of these motors could be influenced by a series of structural modifications. Adjusting the size of atoms X and Y, for example, resulted in a change in the extent of steric interactions between the upper and lower half of the system, thereby either accelerating or decelerating the thermal helix inversion steps.[11] Varying the size of the substituent R also affected the rate of the thermal step, although the result of this modification was counterintuitive: when the size of R on motor **3** was increased, an increase of the rate of the thermal step was observed (Figure 1b).[12,13] In addition to studies which involve influencing the motor function itself, investigations have been performed toward the functioning of these molecular motors in larger systems. So far, second-generation molecular motors have been successfully immobilized on gold nanoparticles[14] and quartz and silica surfaces,[15] used to influence the speed of rotation of an attached secondary rotor,[16] and applied to induce and switch a preference of the helical screw sense of an attached helical polymer.[17] In addition, they were explored as chiral dopants in liquid crystals in order to induce cholesteric phases in a reversible manner and control the helical organization of these mesophases[18] and to induce microscopic rotary motion.[19]

In order to study and harness the unidirectionality of the rotary motion and the intrinsic helical shape of these motors, most of the aforementioned studies required the use of these motors in their enantiopure form. Procedures for the enantioselective synthesis of first-generation molecular motors have previously been developed.[20,21] However, a procedure which can provide enantiomerically pure second-generation motors directly has so far not been available.[22] Second-generation motors have therefore always been synthesized as a racemate, after which preparative chiral stationary phase HPLC (CSP-HPLC) was used to separate the enantiomers. The amount of material that can be separated in a single "run" is usually limited to only a few milligrams. This amount is typically enough to allow the performance of spectroscopic measurements but often insufficient when one would like to examine other material properties or study these molecules in complex systems such as surfaces, polymers, liquid crystals, and Langmuir−Blodgett films. Multiple chiral HPLC runs are needed in these cases, meaning a significant investment in both equipment and solvents as well as time. Additionally, the separation of these molecular motors by CSP-HPLC is often challenging due to the small difference in the retention times of the two enantiomers and their low solubility in the required eluent. Because of these drawbacks, preparative CSP-HPLC is a less attractive method to provide enantiopure motors. Consequently, future research on functional second-generation motors would benefit considerably from a procedure for their enantioselective preparation.

Second-generation molecular motors are usually constructed by connecting an upper-half diazo compound to a

(9) Koumura, N.; Zijlstra, R. W. J.; van Delden, R. A.; Harada, N.; Feringa, B. L. *Nature* **1999**, *401*, 152–155.

(10) (a) Koumura, N.; Geertsema, E. M.; Meetsma, A.; Feringa, B. L. *J. Am. Chem. Soc.* **2000**, *122*, 12005–12006. (b) Koumura, N.; Geertsema, E. M.; van Gelder, M. B.; Meetsma, A.; Feringa, B. L. *J. Am. Chem. Soc.* **2002**, *124*, 5037–5051.

(11) For a comprehensive review, see: Pollard, M. M.; Klok, M.; Pijper, D.; Feringa, B. L. *Adv. Funct. Mater.* **2007**, *17*, 718–729.

(12) (a) Vicario, J.; Meetsma, J.; Feringa, B. L. *Chem. Commun.* **2005**, 5910–5912. (b) Vicario, J.; Walko, M.; Meetsma, A.; Feringa, B. L. *J. Am. Chem. Soc.* **2006**, *128*, 5127–5135.

(13) A similar finding about the effect of substituents on rotational barriers was found by Kelly and co-workers in their research on molecular ratchets increasing the size of the "pawl" of a ratchet lowered the barrier to rotation. Their explanation for this observation is that a larger pawl increases the energy of the ground state of the molecule, thus bringing it closer to the rotation energy barrier. See: Kelly, T. R.; Sestelo, J. P.; Tellitu, I. *J. Org. Chem.* **1998**, *63*, 3655–3665.

(14) van Delden, R. A.; ter Wiel, M. K. J.; Pollard, M. M.; Vicario, J.; Koumura, N.; Feringa, B. L. *Nature* **2005**, *437*, 1337–1340.

(15) Pollard, M. M.; Lubomska, M.; Rudolf, P.; Feringa, B. L. *Angew. Chem., Int. Ed.* **2007**, *46*, 1278–1280.

(16) ter Wiel, M. K. J.; van Delden, R. A.; Meetsma, A.; Feringa, B. L. *Org. Biomol. Chem.* **2005**, *3*, 4071–4076.

(17) Pijper, D.; Feringa, B. L. *Angew. Chem., Int. Ed.* **2007**, *46*, 3693–3696.

(18) (a) van Delden, R. A.; Koumura, N.; Harada, N.; Feringa, B. L. *Proc. Natl. Acad. Sci. U.S.A.* **2002**, *99*, 4945–4949. (b) Eelkema, R.; Feringa, B. L. *Org. Biomol. Chem.* **2006**, *4*, 3729–3745. (c) Eelkema, R.; Feringa, B. L. *Chem. Asian J.* **2006**, *1*, 367–369.

(19) (a) Eelkema, R.; Pollard, M. M.; Vicario, J.; Katsonis, N.; Ramon, B. S.; Bastiaansen, C. W. M.; Broer, D. J.; Feringa, B. L. *Nature* **2006**, *440*, 163. (b) Eelkema, R.; Pollard, M. M.; Katsonis, N.; Vicario, J.; Broer, D. J.; Feringa, B. L. *J. Am. Chem. Soc.* **2006**, *128*, 14397–14407. (c) Bosco, A.; Jongejan, M. G. M.; Eelkema, R.; Katsonis, N.; Lacaze, E.; Ferrarini, A.; Feringa, B. L. *J. Am. Chem. Soc.* **2008**, *130*, 14615–14624.

(20) (a) Harada, N.; Koumura, N.; Feringa, B. L. *J. Am. Chem. Soc.* **1997**, *119*, 7256–7264. (b) Fujita, T.; Kuwahara, S.; Harada, N. *Eur. J. Org. Chem.* **2005**, 4533–4543.

(21) For a catalytic asymmetric synthesis of overcrowded alkenes, see: Hojo, D.; Noguchi, K.; Tanaka, K. *Angew. Chem., Int. Ed.* **2009**, *48*, 8129–8132.

(22) While this paper was under consideration, Tietze *et al.* published an attractive asymmetric catalytic synthesis of chiral overcrowded alkenes that are structurally analogous to second-generation molecular motors. See: Tietze, L. F.; Düfert, A.; Lotz, F.; Sölter, L.; Oum, K.; Lenzer, T.; Beck, T.; Herbst-Irmer, R. *J. Am. Chem. Soc.* **2009**, *131*, 17879–17884.

SCHEME 1. (a) Key Disconnections in the Retrosynthesis of a Second-Generation Molecular Motor, (b) Conversion of an Enantiopure Upper-Half Ketone to the Corresponding Hydrazone with Accompanying Racemization

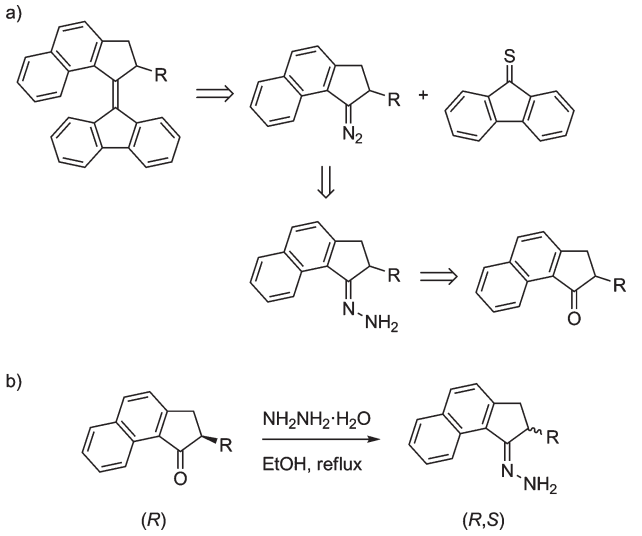

lower-half thioketone through a Barton−Kellogg reaction (Scheme 1a).[23−25] The diazo compound is typically generated in situ by oxidation of the corresponding hydrazone, which in turn can be obtained from the corresponding ketone by treatment with hydrazine. Since the stereogenic center that is situated in the upper half is already present in the ketone precursor, the most straightforward approach for an enantioselective synthesis of the motor would be to prepare the ketone using an enantioselective procedure and then perform the coupling to a lower half without affecting the stereochemistry. However, because of the steric hindrance around the carbonyl group, conversion of the ketone to the hydrazone usually needs to be performed by heating at reflux for several hours. Combined with the basicity of the medium, these conditions allow the ketone to undergo keto−enol tautomerization, causing racemization and thus providing the product hydrazone as a racemate (Scheme 1b).

We anticipated that this racemization could be avoided by converting the ketone to a TBDMS-protected hydrazone by treatment with bis-TBDMS hydrazine and a catalytic amount of scandium(III) triflate. This procedure, introduced by Furrow and Myers,[26] employs much milder conditions than the ordinary hydrazone formation procedure described above as it can be carried out at lower temperatures with short reaction times, whereas the protected hydrazine used in this reaction is a sterically hindered base. Although Furrow and Myers have demonstrated their procedure only with relatively unhindered ketones and aldehydes that were either achiral or not prone to tautomerization, it was anticipated that this procedure would provide the corresponding TBDMS hydrazone from the sterically hindered upper-half

(23) (a) Barton, D. H. R.; Willis, B. J. *J. Chem. Soc. D* **1970**, 1225–1226. (b) Barton, D. H. R.; Smith, B. J.; Willis, B. J. *J. Chem. Soc. D* **1970**, 1226.

(24) (a) Kellogg, R. M.; Wassenaar, S. *Tetrahedron Lett.* **1970**, *11*, 1987–1990. (b) Kellogg, R. M. *Tetrahedron* **1976**, *32*, 2165–2184.

(25) Staudinger, H.; Siegwart, J. *Helv. Chim. Acta* **1920**, *3*, 833–840.

(26) (a) Furrow, M. E.; Myers, A. G. *J. Am. Chem. Soc.* **2004**, *126*, 5436–5445. (b) Furrow, M. E.; Myers, A. G. *J. Am. Chem. Soc.* **2004**, *126*, 12222–12223.

SCHEME 2. Conversion of an Enantiomerically Pure Upper-Half Ketone to the Corresponding TBDMS Hydrazone As a Key Step toward Second-Generation Molecular Motors

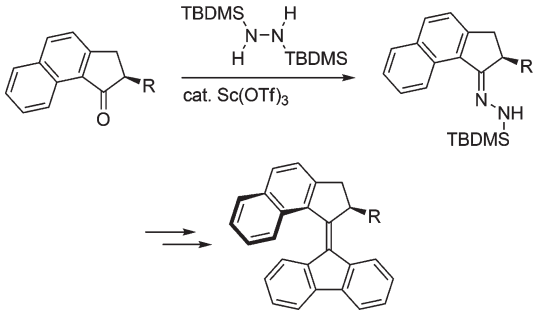

ketone without causing racemization (Scheme 2). After oxidation of the hydrazone to the diazo compound, this compound is then to be used in a Barton−Kellogg coupling procedure during which steps we did not expect any loss of enantiomeric excess (ee).

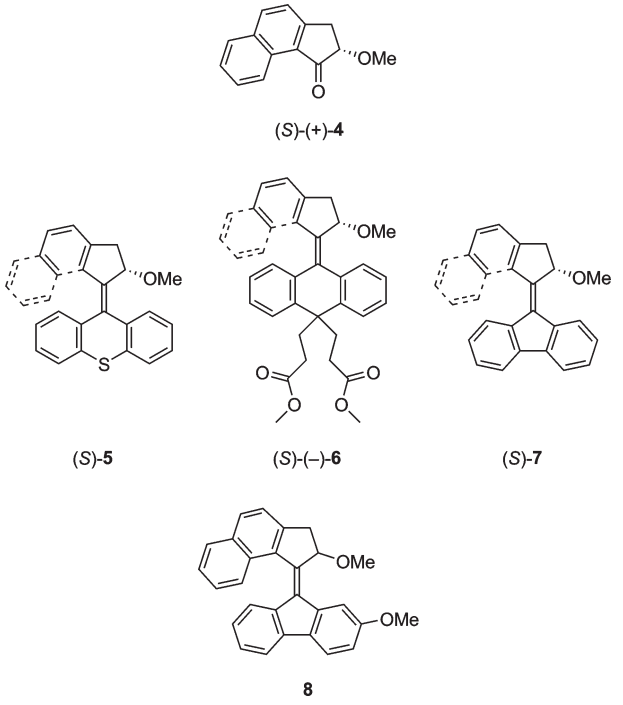

FIGURE 2. Synthesized upper-half ketone (*S*)-**4** and alkenes (*S*)-**5**, (*S*)-**6**, (*S*)-**7**, and **8**.

To test this hypothesis, we have attempted this TBDMS hydrazone formation as well as the subsequent Barton−Kellogg reaction with the enantiomerically enriched ketone (*S*)-**4** (Figure 2). This ketone, which bears a methoxy substituent at the α-position, was prepared via a synthetic route which involved enzymatic kinetic resolution as the key step. In order to obtain the TBDMS-protected hydrazine necessary for the conversion of this ketone to the corresponding TBDMS hydrazone, it proved to be necessary to develop a new, safer procedure to make TBDMS-protected hydrazine. This compound was then used in the preparation of three different second-generation molecular motors, namely, alkenes (*S*)-**5**, (*S*)-**6**, and (*S*)-**7**. As second-generation motors with a methoxy substituent at the stereogenic center

have previously not been made in our laboratories, the photochemical and thermal isomeric behavior of one of these motors, (*S*)-**7**, was studied in detail. Finally, alkene **8**, a desymmetrized version of (*S*)-**7**, was synthesized in order to study the unidirectionality of the rotary motion displayed by this system.

Results and Discussion

The enantioselective synthesis of ketone (*S*)-**4** started from the unsubstituted ketone **9**,[27] which was first converted to an unstable α-hydroxy dimethyl acetal by treatment with [bis(acetoxy)iodo]benzene[28] followed by in situ hydrolysis to provide ketone **10** in 62% yield (Scheme 3). Following a procedure by Saha-Möller and co-workers,[29] enzymatic kinetic resolution was then applied to achieve a selective esterification of the *R* enantiomer,[30] providing the corresponding acetate. The lipase used for this conversion, Amano lipase PS, performed this task with high selectivity, allowing us to obtain ketone (*S*)-**10** in 43% yield out of a maximum theoretical yield of 50%, and with an ee of > 99%. (*S*)-**10** was then treated with silver(I) oxide, iodomethane, and calcium sulfate in order to methylate the hydroxyl function under mild conditions, avoiding racemization and providing ketone (*S*)-**4** in 67% yield and 98% ee.

Bis-TBDMS hydrazine is typically prepared by mixing anhydrous hydrazine and TBDMS chloride, either in the presence or in the absence of a solvent.[26,31] However, as the sale of anhydrous hydrazine in Europe is prohibited and the in-house preparation of anhydrous hydrazine through distillation is very hazardous,[32] we have developed a new procedure for the preparation of bis-TBDMS hydrazine which omits the use of anhydrous hydrazine. In this method, bis-TBDMS hydrazine is prepared from hydrazine monohydrochloride by stirring this compound with TBDMS chloride in the presence of triethylamine at 110 °C for 4.5 h.[33,34] After a quick workup by extraction with *n*-pentane, purification of the crude bis-TBDMS hydrazine is then performed by multiple distillations under reduced pressure. We found that two distillations were enough to provide bis-TBDMS hydrazine that was pure by ^{1}H NMR spectroscopy. However, when the bis-TBDMS hydrazine was subsequently

SCHEME 3. Asymmetric Synthesis of Upper-Half Ketone (*S*)-4

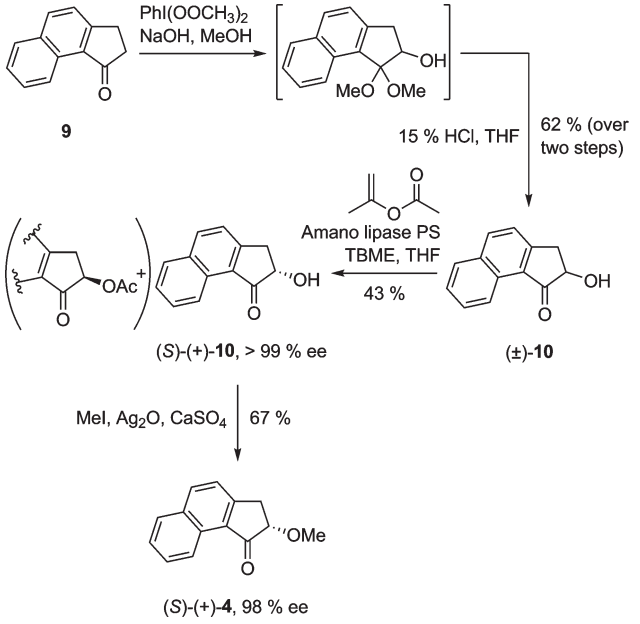

SCHEME 4. Conversion of Ketone (*S*)-4 to TBDMS Hydrazone (*S*)-11

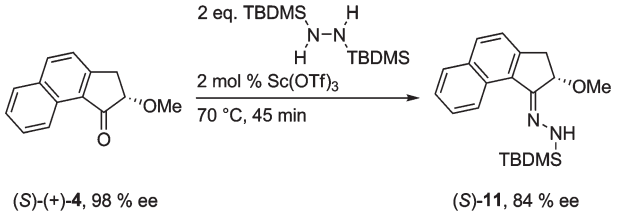

used in the conversion of ketone (*S*)-**4** to the corresponding TBDMS hydrazone (*S*)-**11**, a major drop in ee was observed unless the bis-TBDMS hydrazine was distilled a third time. Additional distillations did not improve the ee any further. Following this method, typically 3.5 g of bis-TBDMS hydrazine (2.4 mL) was isolated from 3.4 g of hydrazine monohydrochloride, which corresponds to a yield of 27%.

Using the three-fold distilled bis-TBDMS hydrazine, ketone (*S*)-**4** was converted to TBDMS hydrazone (*S*)-**11** by heating a mixture of (*S*)-**4**, 2 equiv of bis-TBDMS hydrazine, and 2 mol % of scandium(III) triflate to 70 °C (Scheme 4). The conversion was complete after 45 min, as determined by ^{1}H NMR spectroscopy. Analysis of the reaction mixture with CSP-HPLC revealed that the conversion had proceeded with only limited decrease in enantiopurity, as the ee of (*S*)-**11** was 84%.

Following the progress of the reaction by CSP-HPLC, we observed that the slight decrease of the ee is caused by the gradual racemization of ketone (*S*)-**4** under the reaction conditions: shortly after the reaction had started, the ee of the formed TBDMS hydrazone (*S*)-**11** was 98%; however, as the ee of (*S*)-**4** slowly decreased, so did the ee of (*S*)-**11**. After the completion of the reaction, no further drop in ee was observed, ruling out that TBDMS hydrazone (*S*)-**11** racemizes under the applied reaction conditions.

Two additional investigations have been conducted to determine the cause of the decrease of the ee. First, a mixture

(27) Mayer, F.; Müller, P. *Ber. Dtsch. Chem. Ges.* **1927**, *60*, 2278–2283.
(28) Moriarty, R. M.; Hu, H.; Gupta, S. C. *Tetrahedron Lett.* **1981**, *22*, 1283–1286.
(29) Adam, W.; Díaz, M. T.; Fell, R. T.; Saha-Möller, C. R. *Tetrahedron: Asymmetry* **1996**, *7*, 2207–2210.
(30) The absolute configuration of the enantiomerically pure ketone **10** was assumed to be *S*, based on the substrate preference of Amano lipase PS as reported by Saha-Möller and co-workers.[29] The absolute configuration of ketone **10** (as well as that of the successive compounds ketone **4**, TBDMS hydrazone **11**, and alkenes **5**, **6**, and **7**) was confirmed by X-ray crystallography with refinement of the Flack parameter of alkene **5**.
(31) West, R.; Ishikawa, M.; Bailey, R. B. *J. Am. Chem. Soc.* **1966**, *88*, 4648–4652.
(32) *The Merck Index, An Encyclopaedia of Chemicals, Drugs, and Biologicals*, 13th ed.; O'Neil, M. J., Smith, A., Heckelman, P. E., Budavari, S., Eds.; Merck & Co., Inc.: Whitehouse Station, NJ, 2001; pp 851−852.
(33) The presented procedure does not provide bis-TBDMS hydrazine in a yield better than the procedure of Furrow and Myers,[26] as the formation of bis-TBDMS hydrazine under the described conditions only goes to 80% completion, and at least two distillations are needed to obtain pure bis-TBDMS hydrazine. The presented procedure, however, does not involve the heating of anhydrous hydrazine. Therefore, it can be regarded as a safer alternative, more suitable for the large-scale preparation of bis-TBDMS hydrazine in a laboratory environment.
(34) *Caution*: Although the presented procedure avoids the use of anhydrous hydrazine, suitable safety precautions should still be taken. It is strongly recommended to perform the preparation of bis-TBDMS hydrazine behind a safety blast shield.

TABLE 1. Optimization of the Formation of TBDMS Hydrazone (*S*)-11

entry	bis-TBDMS hydrazine (equiv)	$Sc(OTf)_3$ (mol %)	temp (°C)	(*S*)-**11** (% ee)
1[a]	2	2	70	84
2[a]	2	2	60	84
3[a]	2	2	45	80
4[a]	8	2	70	83
5[a]	8	8	70	84
6[b]	8	0.4	70	77
7[b]	2	0.1	70	80
8[a]	2	40	70	55

[a]Conversion was completed within 45 min. [b]Conversion was completed overnight.

of ketone (*S*)-**4** and 2 equiv of bis-TBDMS hydrazine was stirred overnight at elevated temperature in the absence of scandium(III) triflate. With this experiment, overnight stirring at 70 and 100 °C resulted only in a marginal loss of enantiopurity of (*S*)-**4** (97% ee at 70 °C, 94% ee at 100 °C), far too small to account for the observed decreased ee of (*S*)-**11** since the formation of (*S*)-**11** can be completed in 45 min. However, at 125 °C, the ee of (*S*)-**11** decreased to 23%. A possible explanation for this observation is the disproportionation of the bis-TBDMS hydrazine at this temperature, which would lead to the presence of monoprotected or unprotected hydrazine in the reaction mixture (vide supra). In the second experiment, (*S*)-**4** and 20 mol % of scandium(III) triflate were dissolved in dichloroethane (without bis-TBDMS hydrazine) and stirred at 70 °C. Hereby, we observed a rapid loss of enantiopurity of (*S*)-**4** (50% ee after 3 h). These findings suggest that, under the applied reaction conditions, keto−enol tautomerization catalyzed by the Lewis acid scandium(III) triflate is the major cause of the observed racemization of (*S*)-**4**.[35]

Attempts to optimize the formation of TBDMS hydrazone (*S*)-**11** are summarized in Table 1. Lowering the reaction temperature did not improve the ee of the product (entries 2 and 3) nor did the use of more equivalents of bis-TBDMS hydrazine (entry 4). When both the amount of bis-TBDMS hydrazine and scandium(III) triflate was increased, no change in ee was observed (entry 5). However, an increase in the amount of bis-TBDMS hydrazine combined with a decrease in the amount of scandium triflate resulted in much longer reaction times needed for full conversion as well as a concomitant drop in ee (entry 6). Finally, when the amount of scandium(III) triflate was decreased 20 times, the ee was marginally lower, whereas an increase by the same factor resulted in a substantially lower ee (entries 7 and 8).

Additional attempts to improve the formation of TBDMS hydrazone (*S*)-**11** were made with the use of cosolvents and additives.[36] Two cosolvents, DMF and dioxane, were examined, as we expected that changing the polarity of the reaction medium would have an effect on the interaction between the scandium(III) triflate and ketone (*S*)-**4**. However, with both solvents, no formation of (*S*)-**11** was observed. In another attempt to optimize the TBDMS hydrazone formation, trifluoroacetic acid was used as an additive because it should neutralize any basic impurities formed during the reaction. However, we found that the addition of near-equimolar amounts (0.3 and 0.8 equiv) of trifluoroacetic acid did not lead to an improvement of the ee, and that the use of more trifluoroacetic acid (3 equiv) inhibited the formation of (*S*)-**11**.

Having been able to obtain TBDMS hydrazone (*S*)-**11** in 84% ee, we subsequently employed (*S*)-**11** in the synthesis of three different second-generation molecular motors (Scheme 5). Because of the propensity of second-generation molecular motors as well as their episulfide precursors to crystallize, we expected to be able to readily improve the ee of these motors by crystallization. In each synthesis, the Barton−Kellogg reaction was carried out with a freshly prepared sample of (*S*)-**11**, which had been heated in vacuo at 80 °C for a few hours to remove the bulk of the remaining bis-TBDMS hydrazine as well as most of the TBDMS alcohol that was formed during the reaction.

The Barton−Kellogg reaction of TBDMS hydrazone (*S*)-**11** with thioketone **12**, in which [bis(acetoxy)iodo]benzene was used to convert (*S*)-**11** to the corresponding diazo compound, gave episulfide (*S*)-**13** in 33% yield (based on ketone (*S*)-**4**) and 84% ee, thereby confirming our expectation that this reaction would proceed without any further decrease in ee. Afterward, the easy crystallization of (*S*)-**13** allowed us to raise the ee up to >99% through two consecutive recrystallizations from ethyl acetate. Subsequent desulfurization by treatment with triphenylphosphine provided alkene (*S*)-**5**. (*S*)-**5** was purified by column chromatography using a 9:1 mixture of silica gel and silver nitrate as the stationary phase.[37] In this way, (*S*)-**5** was obtained in 87% yield and >99% ee. X-ray crystallography of (*S*)-**5** with refinement of the Flack parameter was used to confirm that the absolute configuration of the stereogenic center was indeed *S*[30] and that (*S*)-**5** showed an *M* helicity (Figure 3; see also the Supporting Information). Additionally, it was found that the methoxy substituent adopts a pseudoaxial orientation.

Improvement of the ee of the target alkene by recrystallization of the episulfide was also used in the synthesis of alkene (*S*)-**6**, which has two ester chains attached to the lower half, thus allowing this motor to be tethered to a nanoparticle, surface, or another molecule.[14,15] Episulfide (*S*)-**15** was obtained from the coupling reaction of TBDMS hydrazone (*S*)-**11** with thioketone **14**. However, after workup, it was found that we were not able to separate (*S*)-**15** from the remaining thioketone **14** by column chromatography as their R_f was identical under all of the separation conditions examined. To facilitate their separation, we therefore treated crude (*S*)-**15** with hydrazine monohydrate in order to convert the unwanted thioketone to the corresponding hydrazone, after which this hydrazone was easily removed by column chromatography, providing (*S*)-**15** in 56% yield (based on ketone (*S*)-**4**) and 84% ee. (*S*)-**15** was then recrystallized twice from methanol in order to improve the ee up to >99%. Desulfurization by treatment with triphenylphosphine finally provided alkene (*S*)-**6** in 52% yield and >99% ee.

(35) Furrow and Myers screened a broad range of different Lewis acid catalysts and found $Sc(OTf)_3$ to be the most effective; see ref 26.

(36) Furrow and Myers have successfully employed diethyl ether as a cosolvent in some of their reactions to prepare TBDMS-protected hydrazone derivatives.

(37) We were not able to find conditions for the separation of (*S*)-**5** and triphenylphosphine sulfide with regular silica gel or aluminum oxide.

SCHEME 5. Synthesis of Alkenes (*S*)-5, (*S*)-6, and (*S*)-7

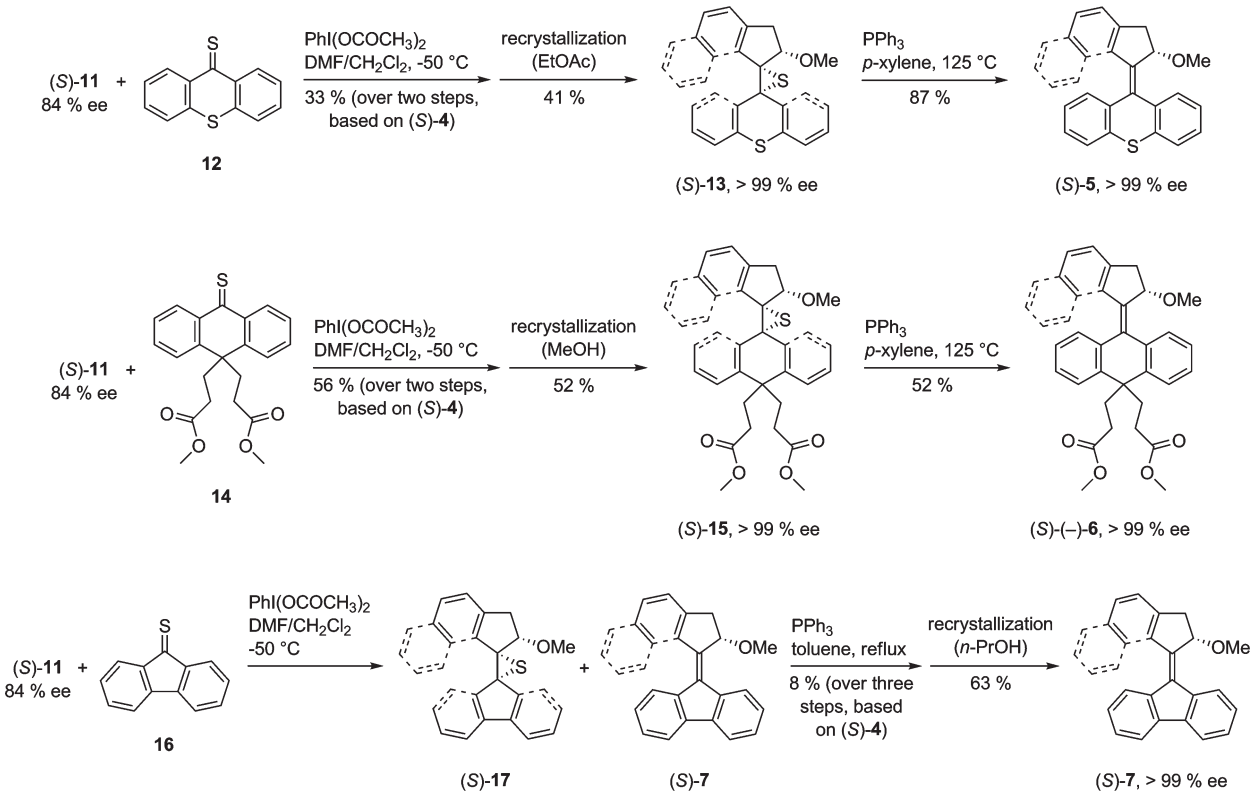

The third second-generation molecular motor that has been successfully prepared using an enantioselective procedure is alkene (*S*)-**7**. This compound was synthesized in order to compare its rotary behavior with that of alkenes **3a**−**d**, hereby elucidating the effect of a methoxy substituent on a motor's rotary action. The Barton−Kellogg reaction was carried out by subsequently treating TBDMS hydrazone (*S*)-**11** with [bis(acetoxy)iodo]benzene and an excess of freshly prepared thioketone **16**, which yielded a mixture of episulfide (*S*)-**17** and alkene (*S*)-**7**. We observed that, during workup and purification by column chromatography, (*S*)-**17** would in part spontaneously desulfurize; therefore, no efforts have been made to isolate and fully characterize (*S*)-**17**. Instead, the mixture was treated with triphenylphosphine in order to desulfurize all of the remaining (*S*)-**17**, providing (*S*)-**7** with 84% ee. During our attempts to purify (*S*)-**7**, we observed that (*S*)-**7** would slowly decompose in the presence of silica gel, which was most likely caused by the acidic nature of silica gel. It was established, however, that the addition of triethylamine to the eluent effectively neutralized the silica gel, thereby minimizing the decomposition of (*S*)-**7** during column chromatography. Finally, the ee of (*S*)-**7** was improved to >99% by a single crystallization from *n*-propanol, which, remarkably, provided nearly racemic crystals and a mother liquor containing enantiomerically pure (*S*)-**7**.

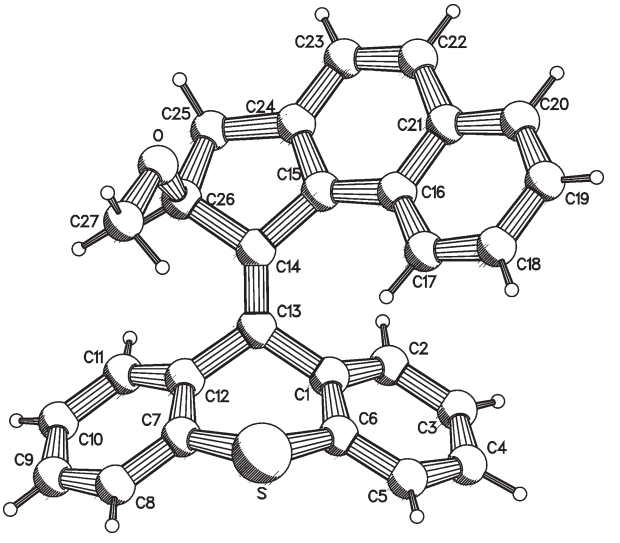

FIGURE 3. Perspective PLUTO drawing of alkene (*S*)-**5**.

As alkene (*S*)-**7** has a symmetric lower half, the first part of a full 360° rotation, comprising one photochemically driven and one thermally driven isomerization step, is identical to the second part, making only two steps of the full rotary cycle distinguishable. In order to enable us to identify by ^{1}H NMR spectroscopy the four distinct steps that make up one full rotary cycle, the lower half of the motor molecule therefore had to be desymmetrized. Toward this goal, alkene **8**, a methoxy-substituted analogue of (*S*)-**7**, was synthesized (Scheme 6). The α-methoxy-substituted ketone **4** was obtained from the unsubstituted ketone **9** by successive formation of the α-hydroxy dimethyl acetal, methylation, and hydrolysis, providing **4** in 62% yield. Ketone **4** was subsequently converted to the corresponding hydrazone **18** by treatment with hydrazine monohydrate at reflux. After formation of the hydrazone had gone to completion, overnight cooling of the reaction mixture at −12 °C

SCHEME 6. Synthesis of Alkenes (*Z*)-8 and (*E*)-8 (Relative Configuration and Helicity Indicated)

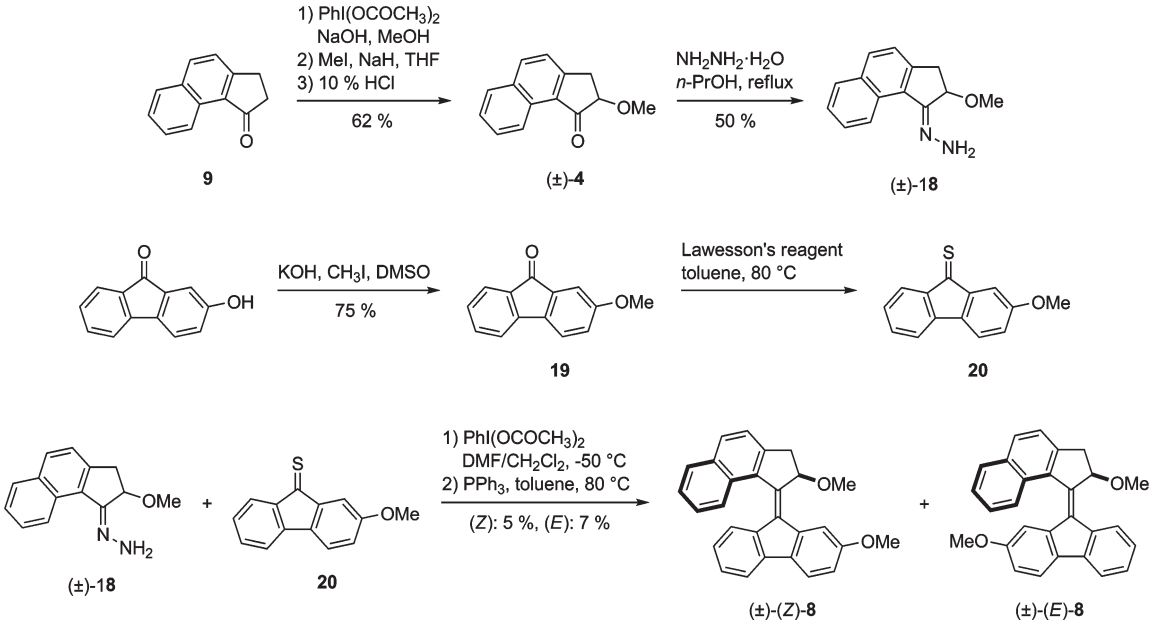

conveniently caused the reaction product to crystallize, providing **18** in 50% yield. Ketone **19** was obtained in 75% yield through the methylation of 2-hydroxyfluorenone by treatment with KOH and iodomethane,[38] after which it was converted to thioketone **20** by treatment with Lawesson's reagent. It was found that when the formation of **20** was performed under reflux conditions the desired product was not obtained, most likely due to degradation of **20** under these conditions.[39] When the reaction temperature was lowered to 80 °C, **20** was obtained, although we found that **20** rapidly decomposed after workup, even when stored at −12 °C. Therefore, this compound was used directly in a Barton−Kellogg reaction with hydrazone **18**.

The Barton−Kellogg reaction of hydrazone **18** and thioketone **20** provided a mixture consisting of two episulfides (the *E*- and *Z*-isomer) and their corresponding alkenes. After workup and filtration over a short column of silica gel, the mixture was directly treated with triphenylphosphine in toluene for 3 h to provide alkenes (*Z*)-**8** and (*E*)-**8**. The purification of these alkenes proved to be challenging as it was observed that, upon column chromatography, these alkenes displayed an even greater extent of degradation on silica gel than their symmetric analogue, alkene (*S*)-**7**. Also, no separation conditions were found when aluminum oxide was used as the stationary phase. It was, however, observed that (*Z*)-**8** and (*E*)-**8** were stable on silica gel TLC plates when a heptane/ethyl acetate mixture was used as the eluent[40] and that preparative silica gel TLC allowed for the complete separation and purification of (*Z*)-**8** and (*E*)-**8**. In this way, (*E*)-**8** was obtained in 7% yield while further purification of (*Z*)-**8** by preparative TLC using a silver nitrate impregnated TLC plate provided (*Z*)-**8** in 5% yield. Alkenes (*E*)-**8** and (*Z*)-**8** were identified by the differences in their ^{1}H NMR spectra: the methoxy groups of (*E*)-**8** are found at 2.78 and 3.05 ppm, whereas those of (*Z*)-**8** are found at 3.03 and 3.59 ppm. Furthermore, (*E*)-**8** has an distinct aromatic proton (the lower half aromatic proton that is spatially the closest to the upper half methoxy substituent) with an absorption at 8.30 ppm, which is shifted downfield from the other aromatic protons.

The photochemical and thermal isomerization processes of alkene (*S*)-**7** were studied by UV−vis and CD spectroscopy (as well as by ^{1}H NMR spectroscopy, vide infra) using a sample of (*S*)-**7** in *n*-hexane (1.1×10^{-5} M) at −20 and −10 °C, respectively. Irradiation at 365 nm resulted in a bathochromic shift of the absorption at 391 nm in the UV−vis spectrum to a slightly broader absorption centered at 402 nm (Figure 4). This spectral change, which we attribute to an increased twist angle of the central olefin, is indicative of the formation of the unstable isomer of (*S*)-**7** by *cis*−*trans* photoisomerization (Scheme 7).[10b,41] The changes in the UV−vis spectrum were accompanied by an inversion of the major absorptions in the CD spectrum (Figure 4), consistent with the inversion of the helicity that is the result of the photochemically induced *cis*−*trans* isomerization. When the samples were subsequently heated, the absorptions in the UV−vis and CD spectra returned to their initial states, which is indicative for the selective conversion of the unstable isomer to the stable isomer by a thermally induced helix inversion (Scheme 7).[10,12]

Characterization of the stable and unstable isomers of alkene (*S*)-**7** by ^{1}H NMR spectroscopy was performed with a sample of stable (*S*)-(*M*)-**7** in toluene-d_8 (Figure 5).[42] First, a ^{1}H NMR spectrum of stable (*S*)-(*M*)-**7** was recorded

(38) Dei, S.; Teodori, E.; Garnier-Suillerot, A.; Gualtieri, F.; Scapecchi, S.; Budriesi, R.; Chiarini, A. *Bioorg. Med. Chem.* **2001**, *9*, 2673–2682.

(39) Scheibye, S.; Shabana, R.; Lawesson, S.-O.; Rømming, C. *Tetrahedron* **1982**, *38*, 993–1001.

(40) We believe that the observed higher stability with TLC silica gel (Analtech UNIPLATE, 2000 μm) could be the result of its higher degree of purity, which would cause it to contain less acidic impurities than silica gel used for column chromatography (SiliCycle SiliaFlash P60, 40−63 μm).

(41) ter Wiel, M. K. J.; van Delden, R. A.; Meetsma, A.; Feringa, B. L. *J. Am. Chem. Soc.* **2003**, *125*, 15076–15086.

(42) The small absorption observed at 4.10 ppm originates from a trace amount of dichloromethane.

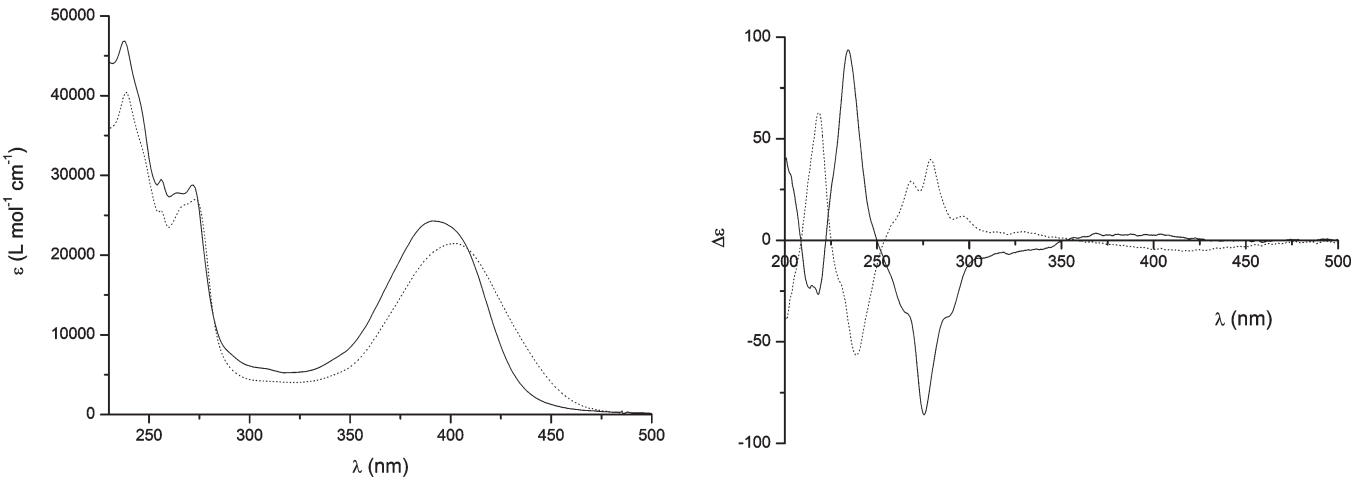

FIGURE 4. UV−vis absorption spectra at −20 °C (left) and CD spectra at −10 °C (right) of alkene (*S*)-**7** in *n*-hexane before (solid) and after (dashed) irradiation at 365 nm.

SCHEME 7. Photochemical *cis*−*trans* Isomerization and Thermal Helix Inversion of Alkene (*S*)-7

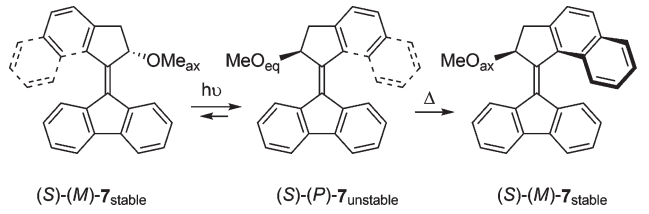

at −30 °C,[43] after which the sample was irradiated overnight at −50 °C. Analysis of the ^{1}H NMR spectrum of the irradiated sample showed, among others, an upfield shift of the −C*H*(OCH$_3$)− signal from 5.36 to 4.88 ppm, corresponding with the expected pseudoaxial to pseudoequatorial conformational change of the methoxy group that takes place during the conversion of the (*S*)-(*M*)-**7** stable isomer to the (*S*)-(*P*)-**7** unstable isomer.[12] The stable/unstable isomer ratio at the photostationary state was determined to be 30:70 by integration of the CH signals of these protons at the stereogenic center. When the irradiated sample was heated to room temperature, the original spectrum was regenerated, indicating a thermal (*S*)-(*P*)-**7** to (*S*)-(*M*)-**7** conversion.

In order to study the kinetic parameters of the thermal helix inversion of alkene (*S*)-**7**, a sample of (*S*)-**7** in *n*-hexane was irradiated at rt until no further change of the UV−vis absorption spectrum was observed. The temperature was then increased, after which the change in absorption at this temperature was monitored at various wavelengths. Using this method, the rate constant (k) of the first-order thermal helix inversion process at 20 °C was determined to be 3.47×10^{-4} s^{-1}, which corresponds to a half-life of 33 min. Comparing this value with that observed for the analogous alkene **3**, it is evident that the rate by which the thermal step of (*S*)-**7** proceeds is decreased compared to that of the methyl-substituted molecular motor **3a** (half-life = 10 min).[12] This behavior fits into the trend that the half-life of the unstable isomers of **3a**−**d** decreases as the relative bulk[11,12,44] of the substituent at the stereogenic center increases. By performing the measurement at temperatures in the range of 20−50 °C, we obtained rate constants for various temperatures. Using an Eyring plot, we found the values of enthalpy of activation ($\Delta H^{\ddagger}$) and entropy of activation ($\Delta S^{\ddagger}$) to be 90 kJ mol^{-1} and −3.8 J mol^{-1} K^{-1}, respectively. The Gibbs free energy of activation ($\Delta G^{\ddagger}$) at 20 °C was calculated to be 91 kJ mol^{-1}.

Careful examination of the ^{1}H NMR spectra of the sample of alkene (*S*)-**7** before irradiation and the same sample after irradiation and subsequent heating revealed that both spectra contain a very small amount of the unstable isomer of (*S*)-**7**, even when the sample is kept in the dark for a long time. Furthermore, we observed by ^{1}H NMR spectroscopy that the amount of unstable isomer increases slightly with temperature, rising from 3% at 20 °C to as much as 5% at 80 °C. These observations imply that the thermal isomerization step, which is typically found to be an irreversible process, is actually reversible with (*S*)-**7**, allowing interconversion between the stable and unstable isomer to a small extent. This implies that the major forward light-driven rotary process is competing with a minor, much slower, backward rotation. A rationale for this finding is that the presence of a methoxy substituent, which is sterically less demanding than the Ph, Me, *i*-Pr, and *t*-Bu substituents that were present on alkene **3**, might lower the energy of the unstable isomer enough to make it thermally accessible. It is not the first time this observation has been made with this type of molecular motor; displacement of the substituent of a second-generation molecular motor from the α-position to the β-position gave a related result.[45] Additionally, directional preference (as opposed to unidirectionality) has also been observed for other motor designs, such as the chemically driven motor reported by our group[7] and the [3]catenane reported by Leigh and co-workers,[8a] and even for the biological rotary motor F_1-ATPase in ATP synthase, which is known to occasionally rotate 120° in the wrong direction.[46] It should be noted that the ^{1}H NMR spectra of alkenes (*S*)-**5** and (*S*)-**6** did not show any unstable isomer, not even at elevated temperatures. This implies

(43) In addition, a 2D NOESY spectrum of (*S*)-(*M*)-**7** was recorded, which can be found in the Supporting Information.

(44) Förster, H.; Vögtle, F. *Angew. Chem., Int. Ed. Engl.* **1977**, *16*, 429–441.

(45) van Delden, R. A.; ter Wiel, M. K. J.; de Jong, H.; Meetsma, A.; Feringa, B. L. *Org. Biomol. Chem.* **2004**, *2*, 1531–1541.

(46) Yasuda, R.; Noji, H.; Kinosita, K., Jr; Yoshida, M. *Cell* **1998**, *93*, 1117–1124.

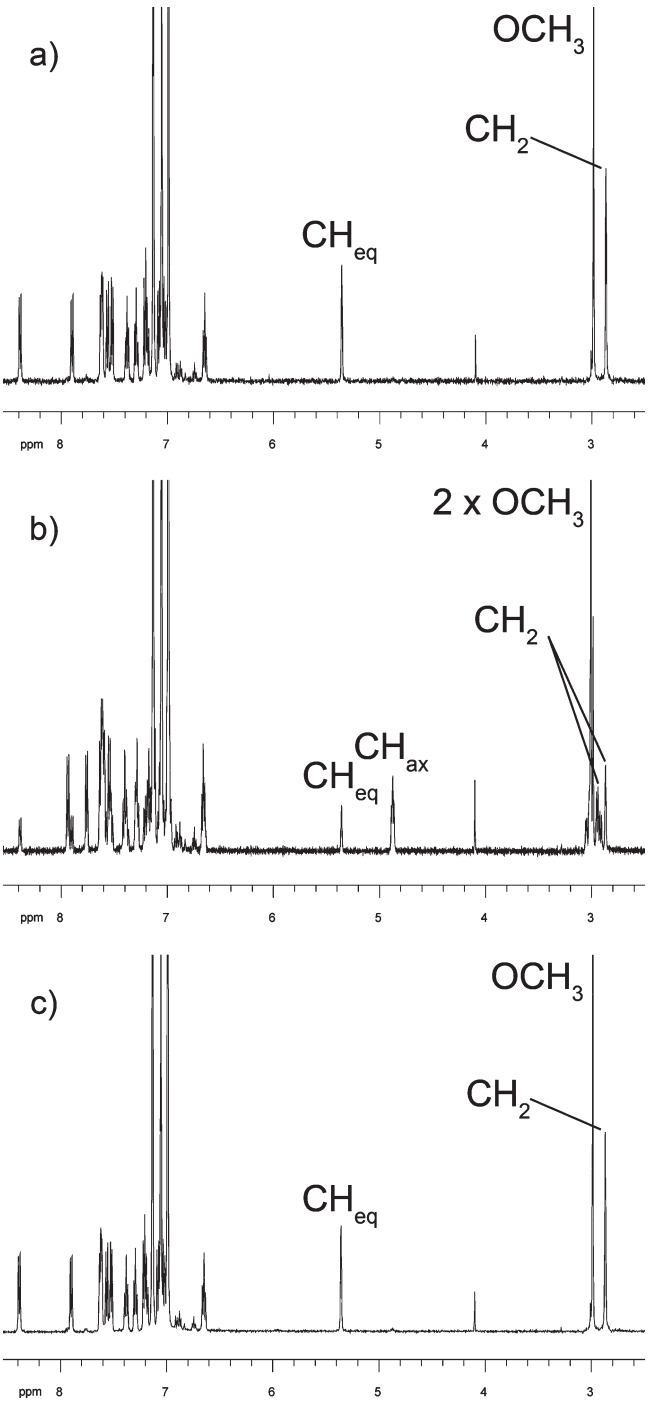

FIGURE 5. Partial ^{1}H NMR spectra of alkene (*S*)-**7** at −30 °C in toluene-d_8 before irradiation (a), after irradiation at 365 nm (b), and after irradiation and subsequent heating (c).

that the minor thermal conversion toward the unstable isomer therefore seems to be a characteristic of only (*S*)-**7** and not of methoxy-substituted second-generation motors in general.[47]

Monitoring of the rotary cycle of the unsymmetrical alkene **8** (Scheme 8) by ^{1}H NMR spectroscopy was

(47) For a recent extensive analysis of unidirectionality, competing processes, and efficiency of rotary motors, see: Geertsema, E. M.; van der Molen, S. J.; Martens, M.; Feringa, B. L. *Proc. Natl. Acad. Sci. U.S.A.* **2009**, *106*, 16919–16924.

SCHEME 8. Rotary Cycle of Alkene 8

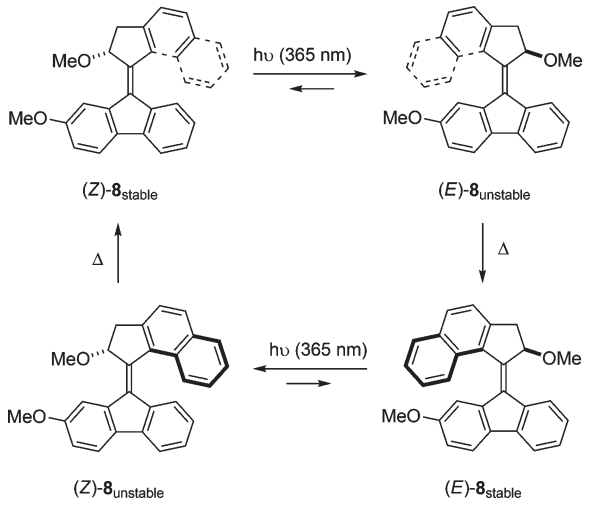

performed in the same way as it was done for alkene **7**.[48] A sample of (*Z*)-**8** in toluene-d_8 was irradiated at −50 °C, showing the formation of the unstable (*E*)-**8** isomer. By integration of the signals of the stereogenic CH of the stable (*Z*)-**8** isomer and unstable (*E*)-**8** isomer at 5.24 and 4.90 ppm, respectively, the ratio of stable/unstable was determined to be 41:59 (at PSS). Minor amounts of stable (*E*)-**8** and unstable (*Z*)-**8** isomers were also observed, indicating, as was observed with alkene **7**, that interconversion between the stable and unstable isomers is possible due to reversibility of the thermal step. The amount of stable (*E*)-**8** and unstable (*Z*)-**8** was, however, relatively small, indicating that **8** still strongly prefers one direction over the other in the overall isomerization pathway. Heating of the sample resulted in the disappearance of the unstable (*E*)-**8** isomer and the appearance of the stable (*E*)-**8** isomer. Irradiation of a sample of (*E*)-**8** led to the formation of the unstable (*Z*)-**8** isomer; however, we also observed that irradiation for a longer period (several hours) caused degradation of these compounds, significantly lowering the intensity of the signals that represent the individual isomers of **8** to the point where these isomers were no longer observed. The stereogenic CH signals of the stable (*E*)-**8** and unstable (*Z*)-**8** were observed at 5.38 and 4.75 ppm, respectively, and on the basis of their integration, the stable/unstable ratio was determined to be 45:55. Heating of the irradiated sample again resulted in the disappearance of the unstable (*Z*)-**8** isomer and the appearance of the stable (*Z*)-**8** isomer. These findings confirm that a 360° unidirectional four-step rotary pathway exists, in which each photochemical isomerization is followed by a thermal isomerization. Although there are minor competing pathways, for the methoxy-substituted motors, the major isomerization processes are photochemical isomerization from stable to unstable forms ($Z \rightarrow E$ and $E \rightarrow Z$) and thermal isomerization from unstable to stable forms ($E \rightarrow Z$ and $Z \rightarrow E$).

Conclusions

Three second-generation light-driven molecular motors were successfully prepared through an enantioselective synthesis. In this route, the enantiomerically enriched

(48) ^{1}H NMR spectra can be found in the Supporting Information.

upper-half ketone (*S*)-**4** was converted to the corresponding TBDMS-protected hydrazone (*S*)-**11** with only a slight drop in ee. We are currently investigating if this approach is also compatible with other upper-half ketones. Preliminary results suggest this might indeed be the case, as an enantiomerically enriched sample of the methyl-substituted analogue of (*S*)-**4**, used as the upper half of molecular motor **3b**, was converted to the corresponding TBDMS-protected hydrazone with nearly complete retention of its stereochemical integrity. As the slight drop in ee could not be avoided, the present approach can only provide enantiomerically pure second-generation molecular motors if the ee can be improved by recrystallization of the target alkene or its episulfide precursor. However, as this class of compounds generally displays a strong propensity to crystallize, improvement of the ee via this method is readily achieved for the majority of these compounds.

Studying the photochemistry of alkene (*S*)-**7** as well as that of its desymmetrized analogue alkene **8**, we found that these compounds display rotational behavior identical to that of earlier reported second-generation molecular motors. However, with the introduction of a methoxy substituent, a limit in the design of these motors seems to have been reached, as the small size and associated steric effect of this methoxy substituent lowers the energy of the unstable isomer far enough to make it thermally accessible. The result of this modification is that the rotary direction displayed by (*S*)-**7** and **8** is not exclusive, but rather a strong preference for directionality is seen. These observations provide important guidelines for the design of future generations of functional molecular motors.

Experimental Section

(±)-2-Hydroxy-2,3-dihydrocyclopenta[*a*]naphthalen-1-one (10). 2,3-Dihydrocyclopenta[*a*]naphthalen-1-one (**9**, 5.00 g, 27.4 mmol) was dissolved in methanol (180 mL) and added dropwise to a solution of KOH (4.60 g, 82.0 mmol) in methanol (75 mL) at 5 °C over a period of 15 min. The mixture was stirred for 10 min and [bis(acetoxy)iodo]benzene (9.60 g, 29.8 mmol) was added in small portions over a period of 10 min, after which the mixture was stirred for 16 h at rt. The majority of the methanol was removed in vacuo. Water (60 mL) was added, and the mixture was extracted with ethyl acetate (2 × 50 mL). The combined organic layers were washed with water (4 × 50 mL), dried over $MgSO_4$, and concentrated in vacuo. The residue was dissolved in THF (20 mL) and acidified with 15% aqueous HCl (40 mL). After stirring for 1 h, the mixture was extracted with ethyl acetate (3 × 30 mL). The combined organic layers were washed with water (4 × 80 mL), dried over $MgSO_4$, and concentrated in vacuo. Purification by column chromatography (silica gel, heptane/ethyl acetate/methanol 12:4:1) yielded ketone (±)-**10** as a yellow solid (3.35 g, 62%): mp 143−145 °C; ^{1}H NMR (400 MHz, CD_2Cl_2) δ 8.93 (d, J = 8.4 Hz, 1H), 8.09 (d, J = 8.4 Hz, 1H), 7.91 (d, J = 8.1 Hz, 1H), 7.67 (dt, J = 8.2, 1.1 Hz, 1H), 7.57 (dt, J = 7.5, 1.1 Hz, 1H), 7.53 (d, J = 8.4 Hz, 1H), 4.57 (dd, J = 7.5, 4.2 Hz, 1H), 3.64 (dd, J = 16.9, 7.3 Hz, 1H), 3.12 (s, 1H), 3.07 (dd, J = 17.0, 4.4 Hz, 1H); ^{13}C NMR (125 MHz, CD_2Cl_2) δ 206.9 (s), 154.4 (s), 136.8 (d), 132.9 (s), 129.3 (s), 129.1 (d), 128.4 (d), 126.9 (d), 124.1 (d), 123.8 (d), 74.3 (d), 35.7 (t), one aromatic (s) was not observed due to overlap with one of the aromatic (d) signals; IR (KBr) 3398, 3057, 2918, 1703, 1518, 1176, 1084 cm^{-1}; m/z (EI, %) 198 (M^+, 100); HRMS (EI) calcd for $C_{13}H_{11}O_2$ 198.0681, found 198.0675.

(*S*)-2-Hydroxy-2,3-dihydrocyclopenta[*a*]naphthalen-1-one (10). Ketone (±)-**10** (1.80 g, 9.08 mmol) was dissolved in a mixture of *tert*-butyl methyl ether (90 mL) and THF (30 mL). Isopropenyl acetate (9.12 g, 91.1 mmol) and Amano lipase PS from *Pseudomonas cepacia* (1.36 g) were added, and the mixture was stirred for 16 h at 22−26 °C. The mixture was subsequently filtered and concentrated in vacuo. Purification by column chromatography (silica gel, heptane/ethyl acetate/methanol 12:4:1) yielded ketone (*S*)-**10** as a yellow solid (781 mg, 43%, > 99% ee): mp 152.7−153.3 °C; $[\alpha]^{20}_D = +132$ (c = 0.33, ethanol). The enantiomeric purity was determined by HPLC analysis (Chiralcel OB-H, heptane/isopropanol 90:10, flow rate = 0.5 mL min^{-1}, t_R = 22.9 min (*R*), t_R = 33.5 min (*S*)).

(*S*)-2-Methoxy-2,3-dihydrocyclopenta[*a*]naphthalen-1-one (4). Ketone (*S*)-**10** (780 mg, 3.68 mmol, > 99% ee) was dissolved in iodomethane (10 mL). Calcium sulfate (2.00 g, 14.7 mmol) and silver(I) oxide (2.45 g, 10.6 mmol) were added, and the resulting mixture was stirred for 16 h at rt. The mixture was filtered, and the residue was washed with acetone, after which the filtrate was concentrated in vacuo. Purification by column chromatography (silica gel, dichloromethane) yielded ketone (*S*)-**4** as an orange solid (561 mg, 67%, 98% ee): mp 60−62 °C; ^{1}H NMR (400 MHz, $CDCl_3$) δ 9.07 (d, J = 8.4 Hz, 1H), 8.08 (d, J = 8.4 Hz, 1H), 7.89 (d, J = 8.1 Hz, 1H), 7.68 (t, J = 7.7 Hz, 1H), 7.57 (t, J = 7.5 Hz, 1H), 7.48 (d, J = 8.4 Hz, 1H), 4.28 (dd, J = 7.3, 4.0 Hz, 1H), 3.70 (s, 3H), 3.59 (dd, J = 17.1, 7.2 Hz, 1H), 3.13 (dd, J = 17.0, 3.9 Hz, 1H); ^{13}C NMR (100 MHz, $CDCl_3$) δ 204.2 (s), 153.8 (s), 136.7 (d), 132.8 (s), 129.3 (s), 129.2 (d), 129.0 (s), 128.3 (d), 126.8 (d), 124.1 (d), 123.8 (d), 81.4 (d), 58.2 (q), 33.6 (t); IR (KBr) 3055, 2930, 2825, 1704, 1518, 1174, 1095 cm^{-1}; m/z (EI, %) 212 (M^+, 25), 182 (100); HRMS (EI) calcd for $C_{14}H_{12}O_2$ 212.0837, found 212.0829; $[\alpha]^{20}_D = +33.5$ (c = 0.33, ethanol). The enantiomeric purity was determined by HPLC analysis (Chiralcel OB-H, heptane/isopropanol 90:10, flow rate = 0.5 mL min^{-1}, t_R = 20.5 min (*R*), t_R = 24.4 min (*S*)).

1,2-Bis(*tert*-butyldimethylsilyl)hydrazine. *Caution: Because of the instable nature of hydrazine, it is strongly recommended to perform this procedure behind a safety blast shield.* Hydrazine monohydrochloride (3.43 g, 50.0 mmol) and *tert*-butyldimethylsilyl chloride (15.1 g, 100 mmol) were placed in a round-bottomed flask equipped with a reflux condenser. Triethylamine (25 mL) was slowly added at rt, after which the mixture was stirred at 110 °C for 4.5 h. During the reaction, additional triethylamine was added after 5, 50, 90, and 140 min (10 mL each time) of reaction time. The mixture was extracted with *n*-pentane (5 × 100 mL), and the combined layers were concentrated in vacuo. The resulting liquid was distilled three times under reduced pressure (85 °C at 1 mmHg), yielding the target hydrazine as a colorless liquid (3.5 g, 27%, 2.4 mL): ^{1}H NMR (400 MHz, $CDCl_3$) δ 2.34 (s, 2H), 0.88 (s, 18H), −0.02 (s, 12H); ^{13}C NMR (100 MHz, $CDCl_3$) δ 26.9 (q), 18.1 (s), −5.6 (q); m/z (EI, %) 260 (M^+, 83), 203 (48), 130 (48), 83 (100); HRMS (EI) calcd for $C_{12}H_{32}N_2Si_2$ 260.2104, found 260.2103.

(*S*)-1-(*tert*-Butyldimethylsilyl)-2-(2-methoxy-2,3-dihydrocyclopenta[*a*]naphthalen-1-ylidene)hydrazine (11). Ketone (*S*)-**4** (40.0 mg, 0.188 mmol, >98% ee), 1,2-bis(*tert*-butyldimethylsilyl)-hydrazine (98 mg, 0.380 mmol), and scandium(III) triflate (1.8 mg, 3.7 μmol) were stirred at 70 °C for 45 min. The mixture was heated in vacuo (1 mmHg) at 80 °C in order to remove the bulk of the remaining bis-TBDMS hydrazine as well as most of the TBDMS alcohol,[49] affording the hydrazone as a mixture of *syn* and *anti* diastereoisomers, which were used in the next reaction step without further purification: ^{1}H NMR (400 MHz, $CDCl_3$) δ 9.30 (d, J = 8.1 Hz, 1H), 7.81 (d, J = 8.1 Hz, 1H), 7.68 (d, J = 8.4 Hz,

(49) It was observed, by ^{1}H NMR, that prolonged concentrating in vacuo at this temperature would lead to partial deprotection of the hydrazone; however, this partial deprotection did not result in lower ee's or yields.

1H), 7.54 (dt, J = 7.5, 1.5 Hz, 1H), 7.46 (dt, J = 7.5, 1.3 Hz, 1H), 7.31 (d, J = 8.1 Hz, 1H), 6.86 (s, 1H), 5.23 (dd, J = 8.1, 3.3 Hz, 1H), 3.44 (dd, J = 18.0, 8.1 Hz, 1H), 3.29 (s, 3H), 3.12 (dd, J = 17.6, 3.3 Hz, 1H), 1.02 (s, 9H), 0.31 (s, 6H, *syn* diastereoisomer), 0.29 (s, 6H, *anti* diastereoisomer); *m*/*z* (EI, %) 340 (M^+, 100), 283 (67), 251 (76); HRMS (EI) calcd for $C_{20}H_{28}N_2OSi$ 340.1971, found 340.1974. The enantiomeric excess (84%) was determined by HPLC analysis (Chiralpak AD, heptane/isopropanol 99.5:0.5, flow rate = 1.0 mL min^{-1}, t_R = 4.6 min (*S*), t_R = 5.6 min (*R*)).

(*S*)-Dispiro[2-methoxy-2,3-dihydro-1*H*-cyclopenta[*a*]naphthalene-1,2′-thiirane-3′,9″-thioxanthene] (13). Hydrazone (*S*)-**11**, freshly prepared from ketone (*S*)-**4** (40.0 mg, 0.188 mmol), was dissolved in DMF (0.5 mL), and the resulting solution was cooled to −50 °C. While stirring, a solution of thioxanthene-9-thione (**14**, 43.0 mg, 0.188 mmol) in a mixture of DMF (0.5 mL) and dichloromethane (0.5 mL) and a solution of [bis(acetoxy)iodo]benzene (60.5 mg, 0.188 mmol) in dichloromethane (0.5 mL) were subsequently added (both solutions were cooled to −50 °C prior to their addition). The mixture was allowed to slowly warm to rt, after which stirring was continued for 1 h. Water (5 mL) was added, and the mixture was extracted with ethyl acetate (2 × 10 mL). The combined organic layers were washed with water (3 × 15 mL), dried over Na_2SO_4, and concentrated in vacuo. Purification by column chromatography (silica gel, toluene) yielded episulfide (*S*)-**13** as a yellow solid (26.4 mg, 33% from ketone (*S*)-**4**, 84% ee). Part of this product (14.8 mg) was recrystallized twice from ethyl acetate, thereby affording episulfide (*S*)-**13** as a white solid (6.1 mg, 13.8% from ketone (*S*)-**4**, >99% ee): mp 212−214 °C; ^{1}H NMR (400 MHz, $CDCl_3$) δ 8.92 (dd, J = 8.8, 2.2 Hz, 1H), 7.92 (dd, J = 7.7, 1.4 Hz, 1H), 7.80 (dd, J = 7.7, 1.1 Hz, 1H), 7.55 (d, J = 8.4 Hz, 1H), 7.51 (dd, J = 6.6, 2.9 Hz, 1H), 7.50 (dd, J = 7.5, 1.3 Hz, 1H), 7.34 (dt, J = 7.5, 1.5 Hz, 1H), 7.21−7.14 (m, 3H), 6.98 (dd, J = 7.7, 1.1 Hz, 1H), 6.93 (dt, J = 7.6, 1.3 Hz, 1H), 6.77 (dt, J = 7.5, 1.5 Hz, 1H), 3.43 (dd, J = 16.3, 4.6 Hz, 1H), 3.25 (s, 3H), 2.95 (d, J = 4.4 Hz, 1H), 2.87 (d, J = 16.5 Hz, 1H), one signal was not observed due to overlap with the solvent signal; ^{13}C NMR (100 MHz, $CDCl_3$) δ 141.4 (s), 138.9 (s), 136.8 (s), 136.1 (s), 134.3 (s), 133.0 (s), 131.4 (s), 131.0 (d), 130.9 (s), 129.8 (d), 128.8 (d), 127.8 (d), 127.3 (d), 127.1 (d), 126.9 (d), 126.89 (d), 126.82 (d), 126.2 (d), 124.9 (d), 124.6 (d), 124.4 (d), 123.3 (d), 86.5 (d), 67.5 (s), 60.8 (s), 57.0 (q), 36.8 (t); *m*/*z* (EI, %) 424 (M^+, 16), 392 (100), 359 (29); HRMS (EI) calcd for $C_{27}H_{20}OS_2$ 424.0956, found 424.0943. The enantiomeric purity was determined by HPLC analysis (Chiralpak AD, heptane/isopropanol 99:1, flow rate = 1.0 mL min^{-1}, t_R = 13.7 min (*S*), t_R = 15.9 min (*R*)).

(*S*)-9-(2′-Methoxy-2′,3′-dihydro-1′*H*-cyclopenta[*a*]naphthalen-1′-ylidene)-9*H*-thioxanthene (5). A solution of episulfide (*S*)-**13** (6.1 mg, 14.4 μmol, >99% ee) and triphenyl phosphine (37.7 mg, 0.144 mmol) in *p*-xylene (1 mL) was stirred for 16 h at 125 °C, after which the mixture was concentrated in vacuo. The crude product was redissolved in dichloromethane (5 mL), and iodomethane (2 mL) was added, after which the mixture was stirred at rt for 1 h. After concentration in vacuo, the residue was filtered over a short column of silica gel that was impregnated with 10% silver nitrate (heptane/ethyl acetate 1:1), concentrated in vacuo, and purified by column chromatography (silica gel, heptane/ethyl acetate 8:1), affording alkene (*S*)-**5** as a white solid (5.0 mg, 87%, >99% ee): mp 156−158 °C; ^{1}H NMR (400 MHz, $CDCl_3$) δ 7.74 (d, J = 8.1 Hz, 1H), 7.70 (d, J = 8.8 Hz, 1H), 7.64 (apparent d, J = 8.1 Hz, 3H), 7.47 (d, J = 8.1 Hz, 1H), 7.38 (dt, J = 7.5, 1.5 Hz, 1H), 7.28 (dt, J = 7.5, 1.3 Hz, 1H), 7.17 (dt, J = 7.3, 1.5 Hz, 1H), 7.06 (dt, J = 7.5, 1.5 Hz, 1H), 6.86−6.79 (m, 2H), 6.75 (dd, J = 7.7, 1.5 Hz, 1H), 6.67 (dt, J = 7.2, 1.1 Hz, 1H), 5.67 (d, J = 4.0 Hz, 1H), 3.61 (dd, J = 15.9, 3.8 Hz, 1H), 3.03 (d, J = 16.1 Hz, 1H), 2.83 (s, 3H); ^{13}C NMR (125 MHz, $CDCl_3$) δ 144.9 (s), 139.5 (s), 139.4 (s), 137.6 (s), 136.0 (s), 135.4 (s), 134.8 (s), 133.7 (s), 133.3 (s), 130.4 (d), 129.0 (d), 128.9 (s), 128.4 (d), 128.1 (d), 127.9 (d), 127.7 (d), 126.9 (d), 126.8 (d), 126.5 (d), 126.36 (d), 126.35 (d), 125.1 (d), 124.4 (d), 123.7 (d), 80.3 (d), 55.3 (q), 39.8 (t); *m*/*z* (EI, %) 392 (M^+, 56), 361 (76), 212 (100); HRMS (EI) calcd for $C_{27}H_{20}OS$ 392.1235, found 392.1238. The enantiomeric purity was determined by HPLC analysis (Chiralpak AD, heptane/isopropanol 99:1, flow rate = 1.0 mL min^{-1}, t_R = 10.7 min (*S*), t_R = 14.0 min (*R*)). The structure and absolute configuration were determined by X-ray crystallographic analysis using Flack's refinement (see Supporting Information).

(*S*)-Dispiro[dimethyl 3,3′-(2-methoxy-2,3-dihydro-1*H*-cyclopenta[*a*]naphthalen-1,2′-thiirane-3′,9″-(9″,10″-dihydroanthracene-9″,9″-diyl)dipropanoate)] (15). Hydrazone (*S*)-**11**, freshly prepared from ketone (*S*)-**11** (40.0 mg, 0.188 mmol), was dissolved in DMF (0.5 mL), and the resulting solution was cooled to −50 °C. While stirring, a solution of dimethyl 3,3′-(10-thioxo-9,10-dihydroanthracene-9,9-diyl)dipropanoate (**14**, 72.0 mg, 0.188 mmol) in a mixture of DMF (0.5 mL) and dichloromethane (0.5 mL) and a solution of [bis(acetoxy)-iodo]benzene (60.5 mg, 0.188 mmol) in dichloromethane (0.5 mL) were subsequently added (both solutions were cooled to −50 °C prior to their addition). The mixture was allowed to slowly warm to rt, after which stirring was continued for 1 h. Water (5 mL) was added, and the mixture was extracted with ethyl acetate (2 × 10 mL). The combined organic layers were washed with water (3 × 15 mL), dried over Na_2SO_4, and concentrated in vacuo. The crude product was redissolved in chloroform (2 mL), and hydrazine monohydrate (0.1 mL) was added, after which the mixture was stirred at rt for 1 min. After concentration in vacuo, the crude product was purified by column chromatography (silica gel, heptane/ethyl acetate 3:1), yielding episulfide (*S*)-**15** as a yellow solid (61 mg, 56% from ketone (*S*)-**4**, 84% ee). This product was recrystallized twice from methanol to afford episulfide (*S*)-**15** as a white solid (32 mg, 29% from ketone (*S*)-**4**, >99% ee): mp 144−145 °C; ^{1}H NMR (400 MHz, $CDCl_3$) δ 9.32 (d, J = 8.8 Hz, 1H), 8.26 (dd, J = 7.9, 1.3 Hz, 1H), 8.05 (dd, J = 7.3, 1.8 Hz, 1H), 7.53−7.32 (m, 6H), 7.24 (t, J = 7.0 Hz, 1H), 7.02−6.99 (m, 2H), 6.93 (dt, J = 7.4, 1.3 Hz, 1H), 6.85 (dt, J = 7.3, 1.3 Hz, 1H), 3.65 (s, 3H), 3.58 (s, 3H), 3.32 (s, 3H), 3.25 (d, J = 5.1 Hz, 1H), 2.93 (dd, J = 17.8, 5.0 Hz, 1H), 2.76 (d, J = 17.6 Hz, 1H), 2.64−2.51 (m, 2H), 2.14−2.07 (m, 1H), 1.86−1.48 (m, 5H); ^{13}C NMR (100 MHz, $CDCl_3$) δ 174.2 (s), 173.3 (s), 142.6 (s), 141.2 (s), 140.7 (s), 137.6 (s), 133.6 (s), 133.4 (s), 132.4 (d), 131.6 (s), 131.3 (s), 129.8 (d), 128.7 (d), 127.9 (d), 127.74 (d), 127.68 (d), 126.3 (d), 125.9 (d), 125.57 (d), 125.55 (d), 124.9 (d), 124.8 (d), 124.3 (d), 123.0 (d), 83.9 (d), 69.4 (s), 60.0 (s), 56.6 (q), 51.7 (q), 51.6 (q), 45.4 (s), 39.0 (t), 36.0 (t), 29.9 (t), 29.4 (t), 29.2 (t); *m*/*z* (EI, %) 578 (M^+, 5), 546 (59), 459 (100); *m*/*z* (CI, NH_3, %) 596 ($M + NH_4^+$, 100), 564 (39); HRMS (EI) calcd for $C_{36}H_{34}O_5S$ 578.2127, found 578.2116. The enantiomeric purity was determined by HPLC analysis (Chiralpak OD, heptane/isopropanol 95:5, flow rate = 1.0 mL min^{-1}, t_R = 12.0 min (*S*), t_R = 26.7 min (*R*)).

(*S*)-Dimethyl-3,3′-(10-(2′-methoxy-2′,3′-dihydro-1′*H*-cyclopenta[*a*]naphthalen-1′-ylidene)-9,10-dihydroanthracene-9,9-diyl)-dipropanoate (6). A solution of episulfide (*S*)-**15** (31.8 mg, 54.9 μmol, >99% ee) and triphenyl phosphine (144 mg, 0.549 mmol) in *p*-xylene (2.2 mL) was stirred for 16 h at 125 °C, after which the mixture was concentrated in vacuo. The crude product was redissolved in dichloromethane (5 mL), and iodomethane (2 mL) was added, after which the mixture was stirred at rt for 1 h. After concentration in vacuo, the residue was filtered over a short column of silica gel (diethyl ether), concentrated in vacuo, and purified by column chromatography (silica gel, heptane/ethyl acetate 3:1). Recrystallization from isopropanol yielded alkene (*S*)-**6** as a yellow solid (16 mg, 52%, >99% ee): mp 173−174 °C; ^{1}H NMR (400 MHz, $CDCl_3$) δ 7.75−7.70 (m, 3H), 7.53−7.47 (m, 3H), 7.39−7.33 (m, 2H), 7.19−7.11 (m, 2H),

6.82−6.73 (m, 3H), 6.60 (dt, J = 7.5, 0.9 Hz, 1H), 5.93 (d, J = 3.7 Hz, 1H), 3.70 (s, 3H), 3.60 (dd, J = 15.6, 3.9 Hz, 1H), 3.50 (s, 3H), 3.03 (d, J = 15.8 Hz, 1H), 2.91−2.76 (m, 2H), 2.85 (s, 3H), 2.67−2.46 (m, 4H), 2.14 (t, J = 8.3 Hz, 2H); ^{13}C NMR (125 MHz, $CDCl_3$) δ 174.4 (s), 173.4 (s), 144.9 (s), 141.54 (s), 139.9 (s), 139.6 (s), 139.4 (s), 138.9 (s), 135.7 (s), 133.3 (s), 132.8 (s), 130.2 (d), 129.0 (s), 128.7 (d), 128.5 (d), 128.3 (d), 127.1 (2d), 126.4 (d), 126.1 (d), 126.0 (d), 125.8 (d), 125.7 (d), 124.7 (d), 124.4 (d), 123.8 (d), 80.53 (d), 56.1 (q), 51.9 (q), 51.8 (q), 47.0 (s), 39.9 (t), 36.7 (t), 30.6 (t), 29.5 (t), 27.6 (t); m/z (EI, %) 546 (M^+, 59), 459 (36), 427 (100); HRMS (EI) calcd for $C_{36}H_{34}O_5$ 546.2406, found 546.2389; $[\alpha]^{20}_D$ = −108 (c = 0.75, CH_2Cl_2). The enantiomeric purity was determined by HPLC analysis (Chiralpak OD, heptane/isopropanol 95:5, flow rate = 1.0 mL min^{-1}, t_R = 16.3 min (S), t_R = 39.5 min (R)).

(*S*)-9-(2′-Methoxy-2′,3′-dihydro-1′*H*-cyclopenta[*a*]naphthalen-1′-ylidene)-9*H*-fluorene (7). Lawesson's reagent (286 mg, 0.707 mmol) was added to a solution of fluoren-9-one (84.9 mg, 0.471 mmol) in toluene (1.5 mL), and the resulting mixture was refluxed for 2.5 h. The mixture was concentrated in vacuo, after which the residue was purified by flash column chromatography (silica gel, pentane/dichloromethane 1:1, R_f = 0.8), thereby affording thioketone **16** as a green solid (48.4 mg, 52%). Hydrazone (*S*)-**11**, freshly prepared from ketone (*S*)-**4** (40.0 mg, 0.188 mmol), was dissolved in DMF (0.5 mL), and the resulting solution was cooled to −50 °C. While stirring, a solution of [bis(acetoxy)iodo]benzene (60.5 mg, 0.188 mmol) in dichloromethane (0.5 mL), cooled to −50 °C, was added. After stirring for 20 s, a solution of thioketone **16** (48.4 mg, 0.247 mmol) in a mixture of DMF (0.5 mL) and dichloromethane (0.5 mL), cooled to −50 °C, was added. While stirring, the mixture was allowed to slowly warm to rt, after which the mixture was stirred for an additional hour. Water (5 mL) was added, and the mixture was extracted with ethyl acetate (2 × 10 mL). The combined organic layers were washed with water (3 × 15 mL), dried over Na_2SO_4, and concentrated in vacuo. Purification by column chromatography (silica gel, toluene/heptane 4:1) yielded 23 mg of a yellow solid, which was identified as a mixture of episulfide (*S*)-**17** (R_f = 0.35) and alkene (*S*)-**7** (R_f = 0.4) by ^{1}H NMR spectroscopy. Episulfide (*S*)-**17**: ^{1}H NMR (400 MHz, $CDCl_3$) δ 9.67 (d, J = 8.4 Hz, 1H), 7.81 (d, J = 8.1 Hz, 1H), 7.71−7.57 (m, 5H), 7.48−7.35 (m, 3H), 7.18 (d, J = 8.1 Hz, 1H), 7.15 (d, J = 8.1 Hz, 1H), 7.08 (t, J = 7.5 Hz, 1H), 6.60 (t, J = 7.7 Hz, 1H), 4.55 (d, J = 4.0 Hz, 1H), 3.57 (s, 3H), 2.77 (d, J = 16.1 Hz, 1H), 2.63 (dd, J = 15.4, 3.3 Hz, 1H); m/z (EI, %) 392 (M^+, 2), 360 (43), 329 (100); HRMS (EI) calcd for $C_{27}H_{20}OS$ 392.1235, found 392.1239. The mixture of episulfide and alkene was dissolved in toluene (2.5 mL) with triphenyl phosphine (150 mg, 0.571 mmol) and refluxed for 16 h, after which the mixture was concentrated in vacuo. The crude product was redissolved in dichloromethane (1 mL), and iodomethane (1 mL) was added, after which the mixture was stirred at rt for 1 h. After concentration in vacuo, the residue was filtered over a short column of silica gel (dichloromethane), concentrated in vacuo, and filtered over a short column of silica gel that was impregnated with 10% silver nitrate (heptane/ethyl acetate 1:1). Purification was performed by column chromatography (silica gel, toluene/heptane 3:1 + 3% triethylamine) and afforded alkene (*S*)-**7** as a yellow oil (5.1 mg, 8% from ketone (*S*)-**4**, 84% ee) with only a minor impurity remaining (visible by ^{1}H NMR spectroscopy in the region of 6.7−7.0 ppm). The compound was crystallized from *n*-propanol, after which the mother liquor was concentrated in vacuo, yielding alkene (*S*)-**7** as a yellow solid (3.2 mg, 5% from ketone (*S*)-**4**, >99% ee); ^{1}H NMR (500 MHz, toluene-d_8) δ 8.35 (d, J = 7.7 Hz, 1H), 7.87 (d, J = 8.5 Hz, 1H), 7.63 (apparent t, J = 7.5 Hz, 2H), 7.59 (d, J = 8.2 Hz, 1H), 7.54 (d, J = 7.5 Hz, 1H), 7.33 (t, J = 7.4 Hz, 1H), 7.27 (t, J = 7.4 Hz, 1H), 7.22 (d, J = 8.4 Hz, 1H), 7.19 (t, J = 7.6 Hz, 1H), 7.06−7.02 (m, 4H), 6.65 (t, J = 7.5 Hz, 1H), 5.43 (d, J = 3.7 Hz, 1H), 3.03 (s, 3H), 2.97 (dd, J = 16.4, 3.7 Hz, 1H), 2.91 (d, J = 16.3 Hz, 1H); ^{13}C NMR (125 MHz, $CDCl_3$) δ 146.3 (s), 142.4 (s), 140.6 (s), 140.4 (s), 139.9 (s), 137.2 (s), 136.5 (s), 135.3 (s), 133.1 (s), 131.5 (d), 129.2 (s), 128.9 (d), 128.1 (d), 128.0 (d), 127.7 (d), 127.6 (d), 127.1 (d), 126.4 (d), 126.3 (d), 125.7 (d), 125.1 (d), 123.6 (d), 119.7 (d), 119.4 (d), 87.1 (d), 54.5 (q), 38.1 (t); m/z (EI, %) 360 (M^+, 46), 329 (100); HRMS (EI) calcd for $C_{27}H_{20}O$ 360.1514, found 360.1496. The enantiomeric purity was determined by HPLC analysis (Chiralpak OD, heptane/isopropanol 99:1, flow rate = 1.0 mL min^{-1}, t_R = 10.6 min (S), t_R = 12.5 min (R)).

(±)-2-Methoxy-2,3-dihydrocyclopenta[*a*]naphthalen-1-one (4). 2,3-Dihydrocyclopenta[*a*]naphthalen-1-one (**9**, 4.22 g, 23.2 mmol) was dissolved in methanol (115 mL) and added dropwise to a solution of KOH (3.90 g, 69.5 mmol) in methanol (60 mL) over a period of 15 min at 5 °C. The mixture was stirred for 10 min, and [bis(acetoxy)iodo]benzene (8.10 g, 25.1 mmol) was added in small portions over a period of 10 min, after which the mixture was stirred for 16 h at rt. The majority of the methanol was removed in vacuo. Water (100 mL) was added, and the mixture was extracted with ethyl acetate (2 × 75 mL). The combined organic layers were washed with water (4 × 50 mL), dried over $MgSO_4$, and concentrated in vacuo. The residue was dissolved in THF (30 mL) and cooled to 0 °C, after which sodium hydride (1.10 g, 45.8 mmol) was added. After the resulting mixture was stirred for 5 min, methyl iodide (1.4 mL) was added and stirring was continued for 16 h. The mixture was acidified with 10% aqueous HCl (50 mL) and stirred for 3 h, after which it was extracted with ethyl acetate (3 × 30 mL). The combined organic layers were washed with water (4 × 80 mL), dried over $MgSO_4$, and concentrated in vacuo. Purification by column chromatography (silica gel, heptane/ethyl acetate/methanol 12:4:1) yielded ketone (±)-**4** as a yellow solid (3.05 g, 62%): mp 85.8−86.1 °C.

(±)-(2-Methoxy-2,3-dihydrocyclopenta[*a*]naphthalen-1-ylidene)-hydrazine (18). Ketone (±)-**4** (1.00 mg, 4.71 mmol) was dissolved in a stirred mixture of hydrazine monohydrate (10 mL) and *n*-propanol (10 mL) and heated to reflux for 24 h. Stirring was ceased, and the mixture was cooled to −12 °C, thereby allowing the product to crystallize from the reaction mixture. Filtration afforded hydrazone (±)-**18** as brown solid (536 mg, 50%): mp 76−78 °C; ^{1}H NMR (400 MHz, $CDCl_3$) δ 9.19 (d, J = 8.4 Hz, 1H), 7.83 (d, J = 8.1 Hz, 1H), 7.76 (d, J = 8.4 Hz, 1H), 7.57 (dt, J = 7.7, 1.1 Hz, 1H), 7.48 (dt, J = 7.3, 1.1 Hz, 1H), 7.34 (d, J = 8.4 Hz, 1H), 6.26 (s, 2H), 5.16 (dd, J = 7.0, 2.6 Hz, 1H), 3.49 (dd, J = 17.4, 7.5 Hz, 1H), 3.42 (d, J = 1.5 Hz, 3H), 3.15 (dd, J = 17.6, 3.3 Hz, 1H); ^{13}C NMR (100 MHz, $CDCl_3$) δ 153.9 (s), 142.4 (s), 133.0 (s), 131.1 (s), 129.8 (d), 128.5 (s), 128.1 (d), 127.0 (d), 125.51 (d), 125.50 (d), 123.1 (d), 77.0 (d), 54.3 (q), 34.8 (t); IR (KBr) 3402, 3300, 3240, 3051, 2931, 2823, 1701, 1597, 1514, 1196, 1086 cm^{-1}; m/z (EI, %) 226 (M^+, 100), 165 (96); HRMS (EI) calcd for $C_{14}H_{14}N_2O$ 226.1106, found 226.1105.

2-Methoxyfluoren-9-one (19). KOH (286 mg, 5.10 mmol) was grounded and suspended in dimethyl sulfoxide (2.5 mL). After stirring for 10 min, 2-hydroxyfluoren-9-one (250 mg, 1.27 mmol) and iodomethane (0.25 mL) were added and stirring was continued for 20 min. Water (10 mL) was added, and the resulting mixture was extracted with dichloromethane (2 × 10 mL). The combined organic layers were washed with water (2 × 10 mL), dried over Na_2SO_4, and concentrated in vacuo. Purification by column chromatography (silica gel, pentane/dichloromethane 1:1) yielded ketone **19** as a orange solid (200 mg, 75%): mp 78.7−79.0 °C; ^{1}H NMR (400 MHz, $CDCl_3$) δ 7.59 (d, J = 7.3 Hz, 1H), 7.44−7.38 (m, 3H), 7.21−7.18 (m, 2H), 6.97 (dd, J = 8.1, 2.2 Hz, 1H), 3.85 (s, 3H); ^{13}C NMR (100 MHz, $CDCl_3$) δ 193.6 (s), 160.7 (s), 144.7 (s), 136.7 (s), 135.7 (s), 134.7 (d), 134.1 (s), 127.7 (d), 124.1 (d), 121.2 (d), 119.9 (d), 119.5 (d), 109.3 (d), 55.5 (q); IR (KBr) 3055, 2937, 2835, 1716, 1603, 1230

cm^{-1}; *m*/*z* (EI, %) 210 (M^+, 100); HRMS (EI) calcd for $C_{14}H_{10}O_2$ 210.0681, found 210.0670.

(±)-(*E*)-2-Methoxy-9-(2′-methoxy-2′,3′-dihydro-1′*H*-cyclopenta[*a*]naphthalen-1′-ylidene)-9*H*-fluorene (8). Lawesson's reagent (335 mg, 0.829 mmol) was added to a solution of ketone **19** (116 mg, 0.552 mmol) in toluene (2 mL), and the resulting mixture was stirred at 80 °C for 3 h. The mixture was concentrated in vacuo, after which the residue was filtered over a column with silica gel (pentane/dichloromethane 1:1, $R_f = 0.8$) to provide a red oil which contained thioketone **20**. Hydrazone (±)-**18** (50.0 mg, 0.221 mmol) was dissolved in DMF (0.5 mL), and the resulting solution was cooled to −50 °C. While stirring, a solution of [bis(acetoxy)iodo]benzene (71.2 mg, 0.221 mmol) in dichloromethane (0.5 mL), cooled to −50 °C, was added. After stirring for 20 s, a solution of the crude thioketone **20** in a mixture of DMF (0.5 mL) and dichloromethane (0.5 mL), cooled to −50 °C, was added. While stirring, the mixture was allowed slowly to warm to rt, after which the mixture was stirred for an additional hour. Water (5 mL) was added, and the mixture was extracted with ethyl acetate (2 × 10 mL). The combined organic layers were washed with water (3 × 15 mL), dried over Na_2SO_4, and concentrated in vacuo. After filtration over a short column of silica gel (toluene), the resulting oil and triphenyl phosphine (175 mg, 0.753 mmol) were dissolved in toluene (3 mL) and the mixture wsa stirred at 80 °C for 3 h, followed by concentration in vacuo. The crude product was redissolved in dichloromethane (1 mL), and iodomethane (1 mL) was added, after which the mixture was stirred at rt for 1 h. After concentration in vacuo, the residue was filtered over a short column of silica gel (dichloromethane), concentrated in vacuo, and filtered over a short column of silica gel that was impregnated with 10% silver nitrate (heptane/ethyl acetate 1:1). Purification and separation of the diastereomers was performed by preparative TLC (silica gel, hexane/ethyl acetate 20:1 + 0.1% triethylamine), thereby affording alkene (±)-(*E*)-**8** as a yellow oil (5.9 mg, 7%): ^{1}H NMR (500 MHz, toluene-d_8) δ 8.30 (d, J = 6.4 Hz, 1H), 7.84 (d, J = 8.3 Hz, 1H), 7.60−7.55 (m, 3H), 7.43 (d, J = 8.3 Hz, 1H), 7.30−7.25 (m, 2H), 7.21 (d, J = 8.1 Hz, 1H), 7.12 (t, J = 6.8 Hz, 1H), 7.00 (d, J = 8.1 Hz, 1H), 6.83 (dd, J = 8.2, 2.3 Hz, 1H), 6.53 (d, J = 2.4 Hz, 1H), 5.46 (d, J = 3.9 Hz, 1H), 3.05 (s, 3H), 2.97 (dd, J = 16.5, 4.0 Hz, 1H), 2.92 (d, J = 16.4 Hz, 1H), 2.78 (s, 3H); ^{13}C NMR (125 MHz, toluene-d_8) δ 159.2 (s), 146.6 (s), 142.7 (s), 141.2 (s), 140.3 (s), 138.9 (s), 136.9 (s), 136.2 (s), 134.2 (s), 133.2 (s), 131.2 (d), 129.1 (s), 129.0 (d), 128.3 (d), 128.2 (d), 127.2 (d), 126.5 (d), 125.7 (d), 125.5 (d), 123.4 (d), 120.3 (d), 119.2 (d), 116.2 (d), 110.8 (d), 86.6 (d), 53.9 (q), 53.5 (q), 38.2 (t); *m*/*z* (EI, %) 390 (M^+, 57), 359 (100).

(±)-(*Z*)-2-Methoxy-9-(2′-methoxy-2′,3′-dihydro-1′*H*-cyclopenta[*a*]naphthalen-1′-ylidene)-9*H*-fluorene (8). After separation of the diastereomers by preparative TLC as described above, additional purification was performed by preparative TLC using a silica gel TLC plate that was impregnated with 10% silver nitrate (hexane/ethyl acetate 8:1 + 0.1% triethylamine), thereby affording alkene (±)-(*Z*)-**8** as a yellow oil (4.2 mg, 5%): ^{1}H NMR (500 MHz, toluene-d_8) δ 7.94 (d, J = 2.2 Hz, 1H), 7.91 (d, J = 8.6 Hz, 1H), 7.64 (d, J = 8.1 Hz, 1H), 7.60 (d, J = 8.1 Hz, 1H), 7.52 (d, J = 8.2 Hz, 1H), 7.48 (d, J = 7.5 Hz, 1H), 7.23 (d, J = 8.2 Hz, 1H), 7.19 (t, J = 7.2 Hz, 1H), 7.07−7.03 (m, 2H), 6.96−6.93 (m, 2H), 6.61 (t, J = 7.3 Hz, 1H), 5.37 (d, J = 4.0 Hz, 1H), 3.59 (s, 3H), 3.03 (s, 3H), 2.98 (dd, J = 16.6, 4.1 Hz, 1H), 2.92 (d, J = 16.3 Hz, 1H); ^{13}C NMR (125 MHz, toluene-d_8) δ 160.4 (s), 146.5 (s), 142.7 (s), 142.1 (s), 141.3 (s), 137.0 (s), 136.2 (s), 134.1 (s), 133.3 (s), 131.4 (d), 129.5 (s), 128.2 (d), 128.0 (d), 127.2 (d), 126.5 (d), 125.7 (d), 125.4 (d), 123.3 (d), 120.5 (d), 118.9 (d), 114.7 (d), 111.2 (d), 87.1 (d), 55.1 (q), 53.5 (q), 38.0 (t), two signals were not observed due to overlap with the solvent signal; *m*/*z* (EI, %) 390 (M^+, 52), 359 (100); HRMS (EI) calcd for $C_{28}H_{22}O_2$ 390.1620, found 390.1618.

CD Monitoring of the Rotary Cycle. A molar CD spectrum of alkene (*S*)-**7** in *n*-hexane (1.1×10^{-5} M) was taken at −10 °C before and after irradiation at 365 nm, thereby showing formation of the unstable isomer through *cis*−*trans* isomerization by inversion of the CD signal. When the sample was warmed to rt, another inversion of the CD signal was observed and the original spectrum was regained, indicating the formation of the stable isomer. (*S*)-**7**: λ_{max} [nm] ($\Delta\varepsilon$ [L mol^{-1} cm^{-1}]) (*S*)-$\mathbf{7}_{st}$, 218 (−26.7), 234 (+93.7), 275 (−85.9); (*S*)-$\mathbf{7}_{unst}$, 218 (+62.9), 239 (−56.6), 268 (+29.1), 279 (+39.8).

UV Monitoring of the Rotary Cycle. A molar UV spectrum of alkene (*S*)-**7** in *n*-hexane (1.1×10^{-5} M) was taken at −20 °C before and after irradiation at 365 nm, thereby showing formation of the unstable isomer through *cis*−*trans* isomerization by a bathochromic shift of the absorption spectrum. When the sample was warmed to rt, the original spectrum was regained, indicating the formation of the stable isomer: λ_{max} [nm] (ε [L mol^{-1} cm^{-1}]): $\mathbf{7}_{st}$, 391 (25 800); $\mathbf{7}_{unst}$, 402 (22 300).

Determination of the Kinetic Parameters of the Thermal Helix Inversion by UV Monitoring. A sample of alkene (*S*)-**7** in *n*-hexane (1.1×10^{-5} M) was irradiated at 365 nm at rt until the PSS was reached. The sample was inserted into the sample holder of the UV spectrometer, which had been kept at a temperature of 20, 30, 40, or 50 °C. The change in the absorption, associated with the conversion of unstable isomer into stable isomer, was monitored over time at 430, 433, 437, 440, 450, and 500 nm. The change in the absorption at 500 nm was used as the baseline. A clear isosbestic point was observed at 407 nm (see Supporting Information).

^{1}H NMR Monitoring of the Rotary Cycle. A sample of (*S*)-**7**, (*E*)-**8**, or (*Z*)-**8** in toluene-d_8 was cooled to −50 °C in an ethanol bath and irradiated overnight at 365 nm. ^{1}H NMR spectra of the sample, taken at −30 °C before and after irradiation, showed the formation of a second compound of which the ^{1}H NMR spectra correspond to that of the unstable isomer, indicating the conversion of stable isomer into unstable isomer. In the case of (*S*)-**7**, subsequent heating of the sample resulted in the regeneration of the original spectrum. In the case of (*Z*)-**8** (or (*E*)-**8**), subsequent heating of the sample resulted in the disappearance of the unstable isomer and the formation of stable (*E*)-**8** (or (*Z*)-**8**). $\mathbf{7}_{st}$: ^{1}H NMR (500 MHz, toluene-d_8) δ 8.39 (d, J = 7.8 Hz, 1H), 7.90 (d, J = 8.6 Hz, 1H), 7.63−7.61 (m, 2H), 7.57 (d, J = 8.1 Hz, 1H), 7.52 (d, J = 7.6 Hz, 1H), 7.38 (t, J = 7.6 Hz, 1H), 7.30 (t, J = 7.5 Hz, 1H), 7.22−7.18 (m, 2H), 7.08 (d, J = 7.8 Hz, 1H), 7.03 (d, J = 8.1 Hz, 1H), 6.65 (t, J = 7.6 Hz, 1H), 5.36 (s, 1H), 2.99 (s, 3H), 2.87 (s, 2H), one aromatic H signal was not observed due to overlap with the solvent signal.

$\mathbf{7}_{unst}$: ^{1}H NMR (500 MHz, toluene-d_8) δ 7.94 (d, J = 8.5 Hz, 1H), 7.76 (d, J = 7.7 Hz, 1H), 7.64−59 (m, 2H), 7.50 (d, J = 7.4 Hz, 1H), 7.40 (t, J = 7.4 Hz, 1H), 7.29 (t, J = 7.1 Hz, 1H), 7.17 (t, J = 7.6 Hz, 1H), 6.66 (t, J = 7.1 Hz, 1H), 4.88 (t, J = 6.2 Hz, 1H), 3.04 (dd, J = 14.8, 4.9 Hz, 1H), 3.01 (s, 3H), 2.93 (dd, J = 15.4, 7.4 Hz, 1H), five aromatic H signals were not observed due to overlap with the solvent signal.

(*E*)-$\mathbf{8}_{st}$: ^{1}H NMR (500 MHz, toluene-d_8) δ 8.35 (d, J = 7.6 Hz, 1H), 7.85 (d, J = 8.5 Hz, 1H), 7.57−7.55 (m, 2H), 7.53 (d, J = 8.1 Hz, 1H), 7.42 (d, J = 8.1 Hz, 1H), 7.35 (t, J = 7.3 Hz, 1H), 7.31 (t, J = 7.2 Hz, 1H), 7.19 (d, J = 8.1 Hz, 1H), 7.10 (t, J = 7.4 Hz, 1H), 6.94−6.89 (m, 2H), 6.59 (d, J = 2.2 Hz, 1H), 5.38 (s, 1H), 3.01 (s, 3H), 2.88 (s, 2H), 2.71 (s, 3H).

(*Z*)-$\mathbf{8}_{unst}$: ^{1}H NMR (500 MHz, toluene-d_8) observed signals δ 7.98 (d, J = 8.2 Hz, 1H), 6.60 (s, 1H), 4.75 (s, 1H), 3.60 (s, 3H), 3.00 (s, 3H).

(*Z*)-$\mathbf{8}_{st}$: ^{1}H NMR (500 MHz, toluene-d_8) δ 7.95 (d, J = 8.4 Hz, 1H), 7.92 (s, 1H), 7.63 (d, J = 8.2 Hz, 1H), 7.57 (d, J = 8.2 Hz, 1H), 7.52 (d, J = 8.2 Hz, 1H), 7.48 (d, J = 7.7 Hz, 1H), 7.23 (d, J = 8.2 Hz, 1H), 7.19 (t, J = 7.4 Hz, 1H), 7.08 (apparent s, 1H), 7.02

(t, $J = 7.8$ Hz, 1H), 6.62 (t, $J = 7.5$ Hz, 1H), 5.24 (s, 1H), 3.54 (s, 3H), 2.97 (s, 3H), 2.87 (s, 2H), two signals were not observed due to overlap with the solvent signal.

(***E***)-**8**$_{unst}$: ^{1}H NMR (500 MHz, toluene-d_8) δ 7.90 (d, overlaps with s signal from (*Z*)-**8**$_{st}$, 1H), 7.74 (d, $J = 7.7$ Hz, 1H), 7.58−7.57 (m, 3H), 7.44 (d, $J = 8.2$ Hz, 1H), 7.37 (t, $J = 7.2$ Hz, 1H), 7.30 (t, $J = 7.3$ Hz, 1H), 6.48 (s, 1H), 4.90 (s, 1H), 3.05 (s, 3H), 3.05−2.97 (m, overlaps with s signals from (*Z*)-**8**$_{st}$ and (*E*)-**8**$_{unst}$, 2H), 2.68 (s, 3H), four signals were not observed due to overlap with the solvent signal.

Acknowledgment. Financial support from The Netherlands Organization for Scientific Research (NWO-CW) and NanoNed is gratefully acknowledged.

Supporting Information Available: General experimental, spectroscopic data for compounds **4**−**8**, **10**, **11**, **13**, **15**, **18**, and **19**, X-ray crystallographic data for alkene **5**, and UV−vis, CD, and ^{1}H NMR spectra of the stable and unstable isomers of alkenes **7** and **8**. This material is available free of charge *via* the Internet at http://pubs.acs.org.